Martin Rödl, BSc

Steam Reforming of LPG for SOFC applications

MASTERARBEIT

zur Erlangung des akademischen Grades

Diplom-Ingenieur

Masterstudium Verfahrenstechnik

eingereicht an der

Technischen Universität Graz

Betreuer

Dipl.-Ing. Dr. techn. Martin Hauth

Univ.-Prof. Dipl.-Ing. Dr. techn. Matthäus Siebenhofer

Institut für Chemische Verfahrenstechnik und Umwelttechnik

Graz, September 2017

Affidavit

I hereby declare that I have authored this thesis independently, that I have not used other than the declared sources/resources and that I have explicitly marked all material that has been quoted either literally or by content from the sources used. The text document uploaded to TUGrazonline is identical to the present master thesis.

…… ……

date signature

EIDESSTATTLICHE ERKLÄRUNG

Ich erkläre an Eides statt, dass ich die vorliegende Arbeit selbstständig verfasst, andere als die angegebenen Quellen/Hilfsmittel nicht benutzt, und die den benutzten.Quellen wörtlich und inhaltlich entnommenen Stellen als solche kenntlich gemachthabe. Das in TUGRAZonline hochgeladene Textdokument ist mit der vorliegendenMasterarbeit identisch.

…… ……

Datum Unterschrift

Acknowledgment

The following master thesis was written based on a cooperation between the AVL List GmbH, the CEET institute of the Graz University of Technology, and the IWT institute of the Graz University of Technology.

I am sincerely grateful to my supervisor Dipl.- Ing. Dr.tech Martin Hauth from the AVL List GmbH, who not only showed great confidence but also provided me with a great deal of support by sharing his knowledge and expertise. I would also like to thank Univ.-Prof. Dipl.-Ing Dr.tech. Matthäus Siebenhofer for providing invaluable guidance throughout this work.

Moreover, I would like to acknowledge the Institute of Thermal Engineering at the Graz University of Technology for their essential contribution and assistance throughout my experimental part.

Finally, my whole felt gratitude goes to my parents. I would never have been able to finish my studies and this master thesis without their continued support and encouragement.

Kurzfassung

Die Masterarbeit mit dem Thema „Dampfreformierung von LPG für SOFC Anwendungen“ soll die bisherigen Forschungsergebnisse die mit den Brennstoffen Diesel und Methan gemacht wurden um LPG (Liquefied Petroleum Gas) erweitern. Die Stationäre SOFC (Solide Oxide Fuel Cell) ist hinsichtlich ihrer Effizienz und ihrer Vielseitigkeit der zu verwendenden Brennstoffe wie zum Beispiel Diesel, Methan oder Biogas allen anderen Systemen überlegen. Da in Ländern wie Japan und Korea keine Gasversorgung mit Erdgas vorhanden ist, besteht ein hohes kommerzielles Interesse an der Verwendung von LPG als Brennstoff. Die Masterarbeit teilt sich in einen Theoretischen Teil, welcher einen wissenschaftlichen Überblick über den Stand der Technik vermittelt und einen Experimentellen Teil. Zusätzlich sollen daraus kritische Prozessparameter für den Betrieb eines Nickelbasierten Katalysators ermittelt werden. Des Weiteren werden durch ein Simulink Simulationsprogramm die theoretischen Grenzen der LPG Reformierung ausgelotet. Besonders die Prozessparameter S/C-Verhältnis (Steam to Carbon Ratio), Raumgeschwindigkeit, Temperatur und Druck sind von großer Bedeutung in Bezug auf Kohlenstoffbildung. Ausgehend von der Literaturrecherche und dem Simulationsprogramm wird eine Testmatrix entwickelt. Im Experimentellen Teil muss als Erstes die nötige Infrastruktur für den Umbau des Prüfstandes auf LPG geschaffen werden, welcher von der AVL bereitgestellt wurde. Weiter gilt es einen störungsfreien Betrieb des Prüfstandes zu gewährleisten, mit einem kontrollierten Aufheizvorgang und einer Aktivierung des Katalysators. Nach der Inbetriebnahmephase kann mit den eigentlichen Tests begonnen werden. Abschließend gilt es die aus der Literatur und der Simulation ermittelten Prozessparameter mit den experimentellen Daten zu vergleichen und daraus Rückschlüsse auf eine stabile Betriebsweise zu erhalten.

Abstract

The following master thesis „Steam-Reforming of LPG for SOFC applications" intends to expand the scientific knowledge of possible fuels for SOFC (solid oxide fuel cell) applications. Whereas previous tests have been conducted with methane and diesel, the tests performed in this thesis use LPG (Liquefied Petroleum Gas). One of the main advantages of Stationary SOFC is their efficiency and flexibility in terms of types of fuels e.g. methane, diesel, biogas or LPG. Given that countries such as Japan and Korea do not have methane readily available, there is a high commercial interest on using LPG as a possible fuel for fuel cells. This master thesis is split in two main parts. The first theoretical section contains a literature review on current technical solutions and the second an experimental part. The review is focused on finding key process parameters for continuous operation of SR of LPG on a nickel based catalyst. The equilibrium stage is modelled by a Simulink computer simulation program to evaluate the best theoretical boundaries of LPG reforming. The S/C-ratio (Steam to carbon ratio), GHSV (gaseous hourly space velocity), temperature and pressure, as will be shown, prove to be the most important parameters, as they have great influence on carbon formation. A test matrix was developed based on the theoretical part and the computer simulation program. For the experimental part the setup had to be adopted for the process setup of LPG . A controlled start up process needed to be launched for a controlled heat up process, and was necessary to activate the catalyst. After the commissioning phase the actual testing phase started. The final section of the master thesis aims at comparing the literature data as well as the data out of the test model program to the experimental data to develop an understanding of the requiremants for a stable and continuous operation of the test rig.

Table of Contents

Abbreviations

AFR	Air fuel ratio
CHP	Combined heat and power system
DMFC	Direct methanol fuel cell
GC	Gas chromatograph
HHV	High heating value
LSM	Lanthan strontium manganate
LPG	Liquefied Petroleum Gas
MFC	Mass flow controller
NDIR	Non-dispersive infrared
OSR	Oxidative steam reforming
PID	Proportional integral derivative
POX	Partial oxidation
ScSZ	Scandium stabilised zirconia
SOFC	Solid oxide fuel cell
SR	Steam reforming
TCD	Thermal conductivity detector
TPO	Temperature programmed oxidation method
WGS	Water gas shift reaction

List of Symbols

η	Efficiency factor	[-]
λ	Air/fuel ratio	[-]
p_v	Vapour pressure	[bar]
V	Voltage	[V]
R	Ideal gas constant	[J/mol K]
F	Farraday constant	[C/mol]
V_N	Nernst Voltage	[mV]
T	Temperature	[K /°C]
n	Order of reaction	[mol]
z	Number of electrons	[-]
Δp	Pressure difference	[bar]
G	Gibbs-Energy	[J/mol]
H	Reaction entropy	[J/mol]
τ	Transiant response time	[sec/min]
X_i	Convertion rate	[-]
S	Selectivity	[-]
Y	Yield	[-]
$\dot{n}$	Mole flow	[mol/s]
V	Volume	[cm^3]
η_{el}	Efficiency factor	[-]
η_{Carnot}	Carnot efficiency factor	[-]
$\eta_{BZ,max}$	Efficiency factor	[-]
$\dot{V}_{Gil}$	Volume flow Gilibrator	[ml/min]
$\dot{V}_{Soll}$	Volume flow	[ml/min]
$\dot{V}_l$	Volume flow	[Nl/h]
M	Molar mass	[g/mol]
W_{el}	Electrical work	[J/mol]
GHSV	Gaseous hourly space velocity	[cm^3/g h]
SV	Space velocity	[1/h]
S/C	Steam to carbon ratio	[-]

x_i	mole fraction	[-]
τ	space time	[s]
C	concentration	[mol/m^3]
E°	standard voltage	[V]
E	ideal voltage	[V]
R	gas constant	[kJ/kmol K]
a_R	activity reactant	[-]
a_P	activity product	[-]
z	number of moles of electrons	[-]
F	Faraday constant	[C/mol]

1. Introduction

At the moment oil is the most important energy carrier. It does not only ensure the mobility of humans and commodities but also constitutes the fundamental resource of the chemical industry. About 70 % of the worldwide oil production is converted to gas and diesel. Due to this one-sided orientation, several problems observed, since fossil fuels are limited. For example, oil has a statistic range of around 54 years and natural gas of around 60 years. Additionally, combustion of fossil fuels leads to a high emission of pollutants, especially of CO_2. This main polluter, causes irreversible changes in climate. As a consequence, the development of more efficient energy carriers and less harmful energy consumption has a top priority [1].

A possible way to achieve this priority, is to use fuel cells, which have been part of extensive research and development in recent years. Improvement of combustion engine in terms of fuel reduction and less emissions cannot overcome the lack of low conversion efficiency. Fuel cells are able to transform chemical energy straight and with high efficiency to electrical energy. Fuel cells are of great benefit as they are not noisy, clean and flexible in terms of up scaling as well as a decentralised energy conversion. These advantages give the fuel cell a supreme position in future energy conversion [1].

The advantage of high efficiency is expressed in the efficiency factor, which is defined as:

$$\eta\mathrm{el} = \frac{\text{usable elektrical energy}}{\text{input of electrical energy}} \qquad \text{Equation 1.1}$$

In comparison to conventional efficiency factors there is no limitation by the Carnot-efficiency factor. Fuel cells are a part of the galvanic elements, one feature is continued supply of reaction partners and continued discharge of reaction products. The straight transformation of chemical energy to electrical energy by bypassing the intermediate step of thermal and mechanic energy led to a

significant increase of the efficiency factor for example for CHP systems by up to 60 % [2].

High temperature fuel cells should be used as a stationary heat and energy supplier to replace block type thermal power stations. The question raised in this matter is how the high temperature fuel cells could be supplied with hydrogen. A possible solution would be to produce hydrogen on site with a pre-reformer unit. That has several advantages in storing hydrogen, which is always compacted due to its high pressures to store reasonable amounts of hydrogen. An additional problem is the tank geometry, which is pre-defined by the high pressure and usually designed for 1400 bar system pressure. There is no existing infrastructure that could supply fuel cell systems with hydrogen. Therefore, an infrastructure would need to be established to supply the systems with hydrogen leading, however, to enormous investment costs. As a result, a pre reforming unit is more cost-efficient [3]. However, it should be taken into consideration that the technology of fuel cells is still at the beginning of its learning curve. The lack of secured knowledge, the lack of experience in the development of whole concepts and the lack of knowledge in solving detailed problems raises major issues.

Considering the aspects above, the aim of this master thesis is the experimental research of steam reforming of LPG for SOFCs. Beginning with literature research about the steam reforming of LPG, fundamental process parameters need to be found that can provide a starting point for the experimental work. To evaluate possible start parameters, a matlab computer model, which simulates the equilibrium at specific temperature, must be modified to the new LPG components to define a carbon free zone.
Carbon formation is one of the major problems in the steam reforming of hydrocarbons. An extensive part of this thesis is dedicated to this issue. After the theoretical part, the actual experimental part follows. The test rig needs to be prepared first for LPG. Later, the evaluated test parameters are tested on the test rig. By the end of this thesis, it should be possible to deduce suitable test parameters, which enable a test run for several hours.

2. State of the art

The following chapter „State of the art" provides a brief overview of the fuel cell technology. It explains the general function of a fuel cell and gives an inside view of how hydrogen can be produced from hydrocarbons. Furthermore, general and explicit problems are mentioned in terms of catalyst deactivation.

2.1 **Types of Fuel Cells**

A fuel cell should not be misunderstood as an energy storage device. It is an electrochemical energy converter that is able to transform chemical energy in electrical energy [4]. Fuel cells achieve high efficiency factors and low emissions. A further advantage is that they work without noise emission because there are no mechanical parts [3].

Over several decades the development continued and up to now five relevant types of fuel cells exit. They differ in operating temperature, electrical efficiency, electrolyte, transported ions, fuels and cell shape. The electrolyte is the governing factor. The following table 2.1 gives an overview of technologies [5], [6].

Table 2.1 Different Types of fuel cells

Types of fuel cells	Fuel Cell	Temperature [°C]	Electrolyte	Trans-portedi-ons	Fuel	η [%]
Alkaline fuel cell	AFC	20 - 120	KOH	OH-	H2	60-70
Proton exchange membrane fuel cell	PEMFC	50 – 125 lt 120-200 ht	Polymermemb-ran	H+	H2	40-60
Phoshoric acid	PAFC	190 - 210	H3PO4	H+	H2	55
Molten carbonate	MCFC	600 - 650	Alcalicarbonat-cast	CO2-	H2, CO2	65
Solid oxide fuel cell	SOFC	600 - 1000	YSZ	O2-	H2, CO	60-65

In this master thesis the focus lays only on fuelling SOFC fuel cells.

2.2 **The Principle function of a fuel cell**

A fuel cell is a galvanic element which is able to convert the chemical energy of a chemical reaction straight into electrical energy and heat. This can be described as „cold" or „silent" combustion. For example, a hydrocarbon containing fuel gas is oxidised with oxygen (O_2) or air to water (H_2O) and carbon dioxide (CO_2). This is an exothermal reaction where heat is released [3].

Fuel gas + oxidant → water + (carbon dioxide) + heat

A fuel cell is composed of two different porous layers, the electrodes (cathode and anode) in contact with an ion conductive layer the electrolyte. The electrolyte separates the two gas spaces. All fuel cells have similar basic operating principles. These electrons, thus are liberated through conversion of the fuel, pass an electric circle, inducing an electrical current in the fuel cell. The anode splits the feed-fuel catalytically into electrons and ions. The electrons which are generated at the anode are passed on to the cathode they are transported by an external circle to the cathode. The ions which are formed at the anode are transported through the electrolyte to the cathode. Air-oxygen is passing over the cathode. The ions and the electrons both formed at the anode are reunited at the cathode, with the third component usually oxygen. In the case of hydrogen conversion, water is formed.

It depends on the fuel cell type what kind of chemical reaction is involved in oxidation or reduction. Even the way in which the ions are transported and how the reaction product water occurs, depends on the fuel cell type [3], [6].

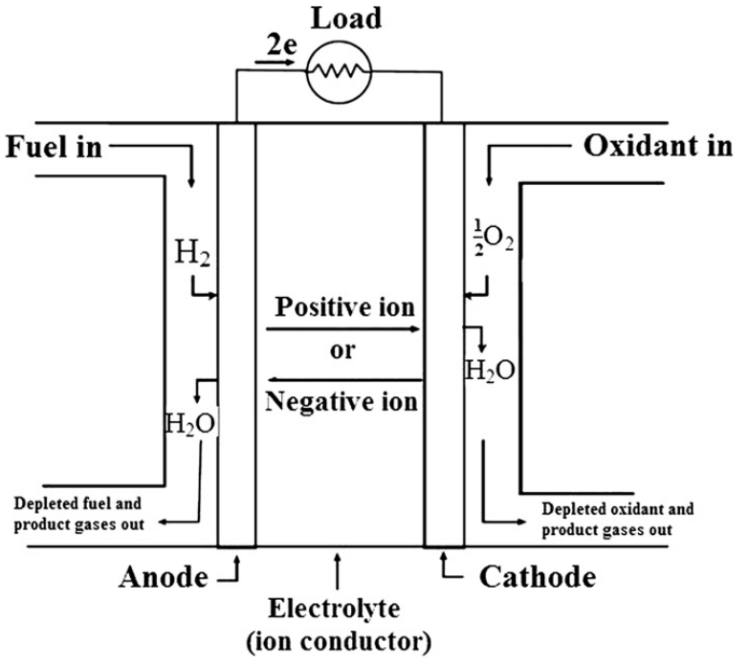

Figure 2.1 Principle of a fuel cell [6]

In the case, of a SOFC fuel cell H_2 reacts with air/oxygen. At the cathode, mobile oxide ions are transported through to the anode, which is unique by SOFC fuel cells. These two reactants and the gross reaction are shown in table 2.2.:

Table 2.2 Electrode reaction SOFC

Anode reaction	$H_2 + O^{2-} \rightarrow H_2O + 2e^-$	Equation 2.1
Cathode reaction	$\frac{1}{2}O_2 + 2e^- \rightarrow O^{2-}$	Equation 2.2
Gross reaction	$H_2 + \frac{1}{2}O_2 \rightarrow H_2O$	Equation 2.3

The gross reaction corresponds to the combustion of hydrogen [3],.

The corresponding Nernst equation for the reaction:

$$E = E^{\circ} - \frac{RT}{nF} * \ln(Q);\ Q = \frac{a_P}{a_R} \qquad \text{Equation 2.4}$$

E° is the standard cell potential, R is the universal gas constant, T is the temperature in Kelvin, F is the Faraday constant, n is the number of electrons transferred per mol of reactant, Q is the term dependant on the activity of reactants (a_R) and product (a_P). The Nernst voltage is the maximum theoretical achievable cell voltage by nonstandard conditions [7].

2.3 **Efficiency factor of SOFC**

The general definition of the efficiency factor of a system is the ratio of the useful output of a system and of the input.

$$\eta = \frac{benefit}{cost} \qquad \text{Equation 2.5}$$

The maximum thermal efficiency factor equation 2.6 of a fuel cell $\eta_{\mathrm{BZ,max}}$ based on the lower heat value is defined as the proportion of the free reaction enthalpy $\Delta_R G$ and the reaction enthalpy $\Delta_R H$.

$$\eta_{BZ,max} = \frac{\Delta_R G}{\Delta_R H} \qquad \text{Equation 2.6}$$

Fuel cells are able to convert the chemical energy straight into electrical energy. This straight way of the transformation process increases the efficiency factor in comparison to steam power plants, since the efficiency factor of the steam power machines is limited by the Carnot efficiency value. The chemical energy is converted in several sub steps to electrical energy.

The Carnot efficiency value depends on the temperature of the heat source T_H and on the temperature of the heat sink T_K .

$$\eta_{Carnot} = \frac{T_H - T_K}{T_H} \qquad \text{Equation 2.7}$$

In a fuel cell it is possible to bypass these limitations because of the straight transformation of the chemical energy into electrical energy.

For hydrogen fuel cells the theoretical maximum efficiency factor can be raised to 94%. The comparison of the two characteristics is shown in figure 2.2.

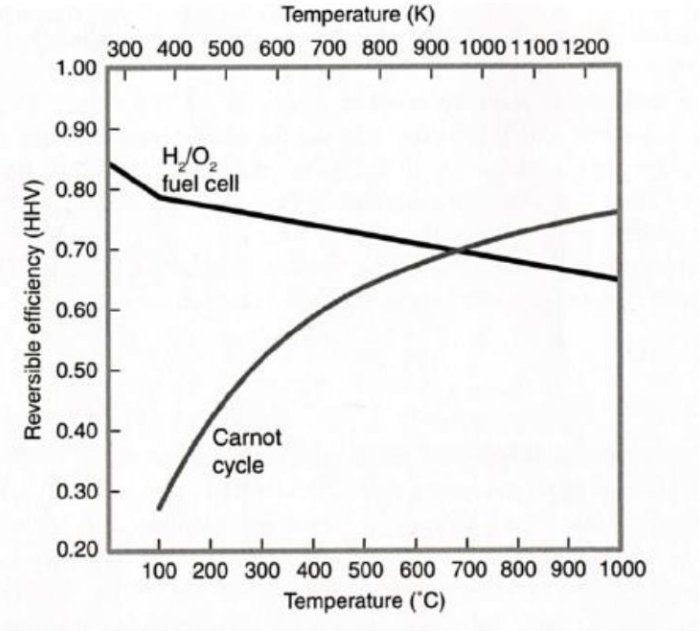

Figure 2.2 Comparison of theoretical reversible HHV hydrogen fuel cell efficiency and Carnot efficiency [7].

The real efficiency factor as a function of energy W_{el} is load dependent. For a SOFC fuel cell stack it is possible to reach a 61 % efficiency factor [8], [9].

2.4 **The operation principle of a SOFC fuel cell**

Like all other fuel cells, SOFC fuel cells are made of an anode (fuel gas), a cathode (air, oxygen) and an electrolyte. The SOFC fuel cell is described as a high temperature fuel cell with an operating temperature between 600°C – 1000°C. This high temperature is necessary to achieve high ion conductivity in the electrolyte and to achieve a reasonable current density. The oxygen ions diffuse to the anode through the electrolyte. By this local surplus of electrons at the anode the voltage in the cell appears, which is developed by a potential difference between anode and cathode.

Since the task is to convert higher hydrocarbons in a synthesis gas atmosphere, the SOFC remains the only option of the available fuel cell types. Additionally, the wide range of operating temperature up to 1000°C in a combination of Ni-anodes makes internal steam reforming of small amounts of hydrocarbons e.g. CH_4, CO_2 or CO hydrogens possible. For higher hydrocarbons, an external pre-reformer is needed [3].

The solid electrolyte in a SOFC is made of ceramic materials and the anode is made of Cobalt Zirconium dioxide (CO-ZrO_2) or Nickel Zirconium dioxide (Ni-ZrO_2).The main difference compared to all other fuel cell types is the oxidation of oxygen on the cathode. The ions diffuse from the cathode to the anode instead of positively charged hydrogen ions travelling from the anode to the cathode. This is unique regarding SOFCs.

The cathode has to be electrically conductive, stable in the oxidative environment and it also reduces the oxygen catalytically. A typical material is Strontium donated Lanthan Manganat (LSM) a semiconductor. There are several designs of SOFCs but in this thesis the focus only lies on planar SOFCs.

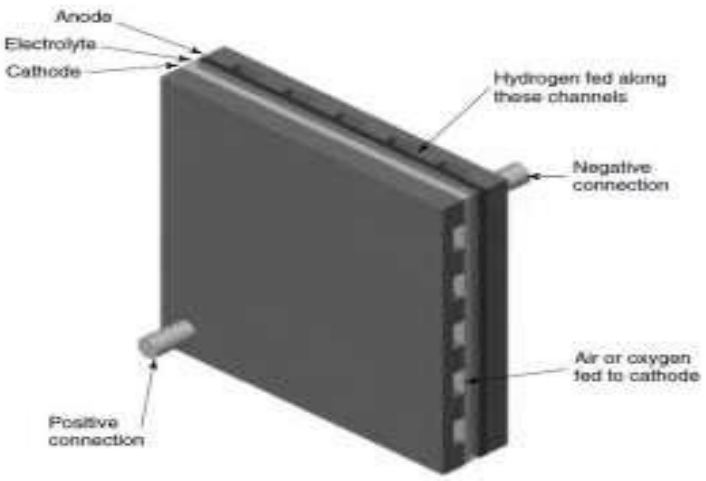

Figure 2.3: Single cell of a stack [10]

The voltage of a single stack layer is about 0.7 V, therefore it is necessary to connect several cells in series to reach an applicable amount of voltage span. Figure 2.4 shows a 3D model of a 30 cell stack.

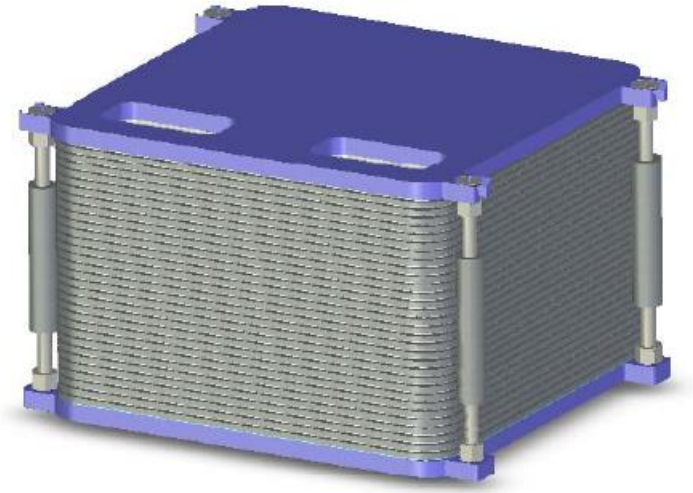

Figure 2.4: Schematic representation of a 3D model of a 30-cell stack [11]

One of the main advantages is the high efficiency factor which adds up to 60% – 65% through the transformation of chemical energy to electrical power. In comparison to the combustion engine, an efficiency factor of 40% can be reached. Also the high exhaust gas temperature can be used for further processes for example to heat the reformer unit [3].

2.5 Methods of Syngas production

Syngas can be produced by a wide range of conventional fuels such as natural gas (methane), methanol, ethanol, dimethyl ether, kerosene, diesel, jet fuels, biodiesel, and mixtures of propane and butane like LPG. These fuels can be reformed to hydrogen rich gas. Alcohol-based fuels can be used as well because they can be reformed at relatively low temperatures and they are free of sulfur compounds [9].

Hydrogen is the most favorable fuel to power the fuel cell, and it can be used in every fuel cell type, as can be seen in chapter 2.1. There are two main ways of producing hydrogen, first through straight oxidation of appropriate fuels and secondly, through steam reforming. The most common way of producing hydrogen is through carbon oxidation with steam reforming [12].

Steam reforming can be realized in two different ways, through:

- Catalytic processing and
- Non-catalytic processing

2.5.1 Types of reforming

As mentioned in chapter 2.5 there are two different ways of steam reforming. The catalytic processing can be subdivided into three main ways:

- Partial Oxidation (POX)
- Oxidative Steam Reforming (OSR)
- Steam Reforming (SR)

The non-catalytic processes are not part of this thesis as they are not widely used and as high temperatures in the range of 600°C - 1000°C lead to unwanted formation of oxides of nitrogen. Additionally, they are very expensive due to their high operating temperature [9].

Partial Oxidation (POX)

The POX is a reaction of hydrocarbons within in oxygen limited atmosphere $\lambda < 1$. The partial oxidation uses the affinity of oxygen to carbon. Due to the lack of oxygen only carbon is oxidised and only free hydrogen is formed.

$$C_nH_m + \frac{n}{2}\,O_2 \leftrightarrow nCO + \frac{m}{2}H_2 \qquad \Delta H°_r < 0 \quad \text{Equation 2.8}$$

POX is an exothermal reaction. The yield depends primary on the air to fuel ratio. The advantages are found in the high flexibility in processable hydrocarbons and in the simple construction [9].

Steam Reforming (SR)

Hydrocarbon reforming with steam, in particular steam reforming of CH_4, is generally the most economic and common way of producing hydrogen. The process of steam reforming hydrocarbon can be expressed by the following chemical reactions [9].

$$C_nH_m + nH_2O \leftrightarrow nCO + \left(\frac{2n+m}{2}\right)H_2 \qquad \Delta H_R° > 0 \qquad \text{Equation 2.9}$$

$$CO + H_2O = CO_2 + H_2O \qquad \text{Equation 2.10}$$

Further explanation of steam reforming of LPG follows in chapter 2.5

Auto thermal Oxidation (ATR)

ATR is a combination of POX and SR. In the best possible scenario the exothermal POX reaction provides the energy for the endothermic SR reaction. So that no external heat supply is necessary. In reality a very precise air and steam supply must hold the process in the operation range of a slightly exothermic area. The process runs in a temperature window of 600°C to 1000°C and S/C-

ratio of 1 - 3 and an air ratio λ between 0.2 - 0.4 depending on the hydrocarbon [9].

It is a combination of both equations POX and SR.

equation 2.8 + equation 2.9

Parallel to this gross reaction from SR and ATR the WGS is taking place.

$$CO + H_2O \leftrightarrow CO_2 + H_2 \qquad \Delta H_r° = -41{,}2\ kJ/mol \qquad \text{Equation 2.11}$$

2.5.2 Steam Reforming of Liquefied Petroleum Gas

Steam reforming is an endotherm equilibrium reaction where hydrocarbons in combination with water steam react on a solid catalyst to carbon monoxide (CO) and hydrogen (H_2) based on the following reaction.

$$C_nH_m + nH_2O \rightarrow nCO + \left(n + \frac{m}{2}\right) H_2 \qquad \Delta H^\circ > 0 \qquad \text{Equation 2.12}$$

Parallel to this reaction, an exothermal WGS reaction takes place, where carbon dioxide (CO_2) and hydrogen (H_2) are finally formed.

$$CO + H_2O \leftrightarrow CO_2 + H_2 \quad \Delta H^\circ = -41{,}2\ kJ/mol \qquad \text{Equation 2.13}$$

The heat balance of the gross reaction is dominated by the reforming reaction equation 2.11 which has a strong exothermic character. Thereby, a supply of thermal energy is needed. The equation 2.11 is only an equilibrium reaction for CH_4. Due to the thermodynamic characteristic of higher hydrocarbons, they tend to be unstable above 350°C, rendering so that equation 2.11 irreversible.

If higher hydrocarbons are converted, an additional methane formation takes place.

$$CH_4 + H_2O \leftrightarrow CO + 3H_2 \qquad \Delta H^\circ = -205{,}6kJ/mol \qquad \text{Equation 2.14}$$

Further reactions can be described during steam reforming, such as dry reforming

$$CH_4 + CO_2 \leftrightarrow 2CO + 2H_2 \qquad \Delta H^\circ = -247kJ/mol \qquad \text{Equation 2.15}$$

and reactions where elementary carbon is formed hydrocarbons dissociate.

$$C_nH_m \rightarrow nC + \frac{m}{2}H_2 \qquad \Delta H^\circ > 0 \qquad \text{Equation 2.16}$$

Boudouard – reaction:

$$2CO \leftrightarrow C + CO_2 \qquad \Delta H^\circ = -172\ kJ/mol \qquad \text{Equation 2.17}$$

Heterogeneous WGS:

$$CO + H_2 \leftrightarrow C + H_2O \qquad \Delta H^\circ = -131\ kJ/mol \qquad \text{Equation 2.18}$$

If all higher hydrocarbons are converted, a chemical equilibrium is achieved with the following products H_2, CO_2, CH_4 and H_2O.

2.6 **Physical and chemical properties of LPG**

Liquefied Petroleum Gas (LPG) is mainly produced in Europe in two different ways. Most of the LPG (around 60%) is produced by natural resources in the upstream production process of wet natural gas and crude oil. About 40% are a by-product of downstream processes. Therefore, the supply chain of Europe's gas supply is directly linked to the availability of the production volume of natural gas and crude oil in the North Sea [1].

In the ÖNORM EN 589 liquefied petroleum gas is generally defined with technical qualities of C_3 and C_4 hydrocarbons propane (C_3H_8), propylene (C_3H_6), butane (C_4H_{10}), butylene (C_4H_8) and mixtures of LPG is not toxic, not soluble in water, which allows the use in protected ground water areas [13].

In this thesis only commercially available LPG is considered because of its simple availability as commonly heating gas. According to ÖNORM EN 589 LPG must be a mixture at minimum 95 Vol. - % propane (C_3H_8) and propylene (C_3H_6) but the amount of propane can differ. The residual can be consist of ethane (C_2H_6), ethylene (C_2H_4), n-butane (C_4H_{10}) and isobutene (C_4H_{10}). The following table 2.3 shows the components of commercially available LPG worldwide.

Table 2.3 Worldwide LPG mixture with the main components propane and butane [14]

Country	Propane [Vol. - %]	Butane [Vol. - %]
Austria	95	5
Belgium	50	50
Denmark	50	50
France	35	65
Greece	20	80
Italy	25	75
Netherlands	50	50
Spain	30	70
Sweden	95	5
United Kingdom	100	-
Germany	90	10
U.S.(HD-5 standard)	85	2,5
Malaysia	40	60
Thailand	60	40
China	30	70

Australia	40	60

In our case the composition of the main components was determined by GC analysis, 97 Vol. - % propane (C_3H_8) and 3 Vol. - % butane (C_4H_{10}) other component have not been tested. LPG is not a standardised gas mixture, and it can differ by its supplier and by origin [15], [14].

The ÖNORM EN 589 defines the allowed sulphur content in liquid gases. The allowed sulphur content determined by 1mg/kg hydrogen sulphide, 5mg/kg dioxide sulphide (SO_2) and elementary sulphur, as well as an odorant mercaptane with a minimum concentration of 4 mg/kg to 5 mg/kg is added. The propane for our tests had a sulphide content of 16 mg/kg, which represents 5 ppm.

2.7 **Gas phase mixture and external effects**

It is possible to liquefy LPG with low pressure in a closed container. The result is a container pressure, which depends on the temperature and the vapour pressure. Figure 2.5 shows the vapour pressure p_v related to the temperature.

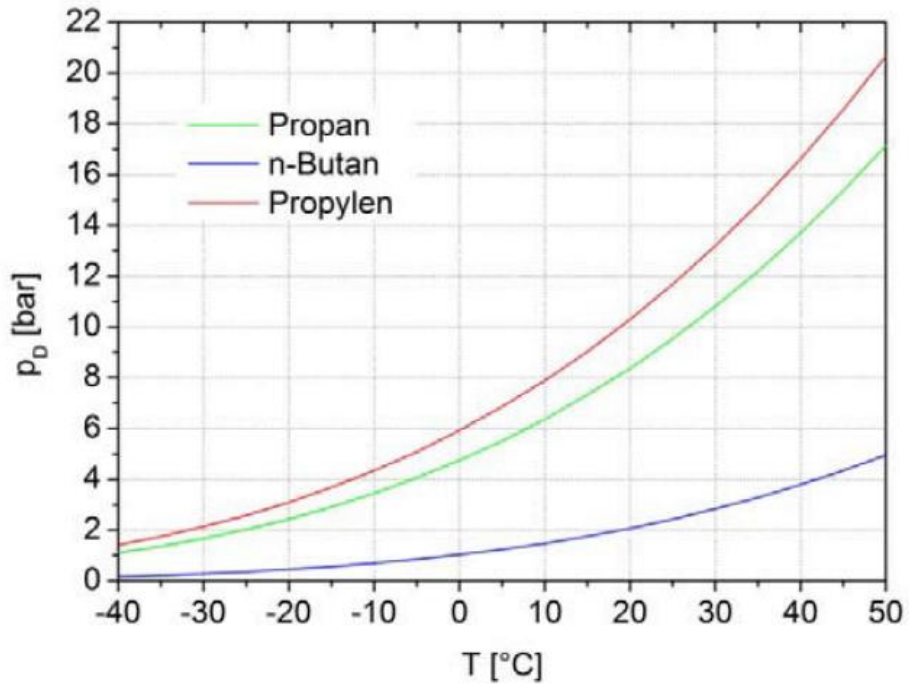

Figure 2.5: vapour pressure curve of propane, n-butane and propylene [15]

The diagram illustrates that the vapour pressure of butane gets close to ambient pressure in mixtures with high contents of butane as a main component, when the mixture are stored outside close to the freezing point. That can cause problems in handling the gas bottles making it almost impossible to take gas out of the bottles. For propane this critical point lies around - 40°C, so there is no problem with supply at low temperatures.

In the case of conventional use of liquefied gas, the amount consumed directly from the gas bottle is so small that the gas components are always at equilibrium. In case of industrial use with high gas flow, equilibrium composition cannot be ensured anymore. Due to high gas flow, the gas bottles cool because of permanent evaporation. Therefore, an additional supply of thermal energy is indispensable.

The vapourpressure of the mixture is different from the vapour pressure of the pure components, which depend on temperature and container volume. Due to continuous relief of the gas phase of a multiple component mixture like LPG, with a liquid fraction and a gas fraction, the concentration above the liquid level changes. At the beginning the gas bottle is full and the amount of low boiling fraction is higher than the amount of high boiling fraction. Through the relief of gas the low boiling fraction is taken out first because of its lighter vapour pressure. The low boiling fraction decreases and the amount of high boiling fraction increases. This results in a change of the composition. The mixture of propane and butane changes according to the filling level of the gas bottle and therefore influences critical process parameters such as the S/C-ratio.

Tests were carried out by *Angerer* [15] a batch distillation simulation program with a mixture of 90 Vol. - % propane (C_3H_8), 5 Vol. - % butane (C_4H_{10}) and 5 Vol. - % of propylene (C_3H_6). As expected the amount of propylene (C_3H_6) and propane (C_3H_8) drops over the gas level but the amount of butane (C_4H_{10}) increases. As a consequence for gas levels less than 10% and 20% the S/C-ratio changes from 4 to 3.84. In the gas level range of 10% to 5% the S/C-ratio changes to 3,71. The author also mentioned that in reality gas tanks are never emptied completely and that most of the time gas tanks are refilled by a gas level of 20% - 25% so the critical level will never be reached. In our case the

amount of propane is higher, namely 97 Vol. - % propane and 1 Vol. - % butane, therefore the change of the mixture occurs at even lower gas levels. Since this phenomenon had been known, the gas bottles were not completely emptied [15].

2.8 System Design of the combined heat and power system

The Chapter system design gives an overview of the whole CHP system. It consists of several main parts, a fuel cell stack (4), an after burner (5), a start-up burner (6), two heat exchangers (1, 2) and a reformer (2). In general, the fuel cell system can be divided into three sub systems. The blue system represents the cathode system, the red line the anode system and the yellow line the pre-treatment of the exhaust gas. The cathode (1) is supplied with air from the heat exchanger (1) where the inlet gas stream is preheated. After the cathode the exhausted gas is feed to the after burner (5) and later to the start burner (6). The start-up burner (6) takes the exhaust gases of the cathode and the anode and supplies the reformer (2) with the heat required. A part of the anode gas is recirculated. The fuel cell (4) is supplied with hydrogen rich gas by the reformer. The entire anode exhaust gas is pre-heated in the heat exchanger (3) to heat up the gas for the anode and the after burner (5).

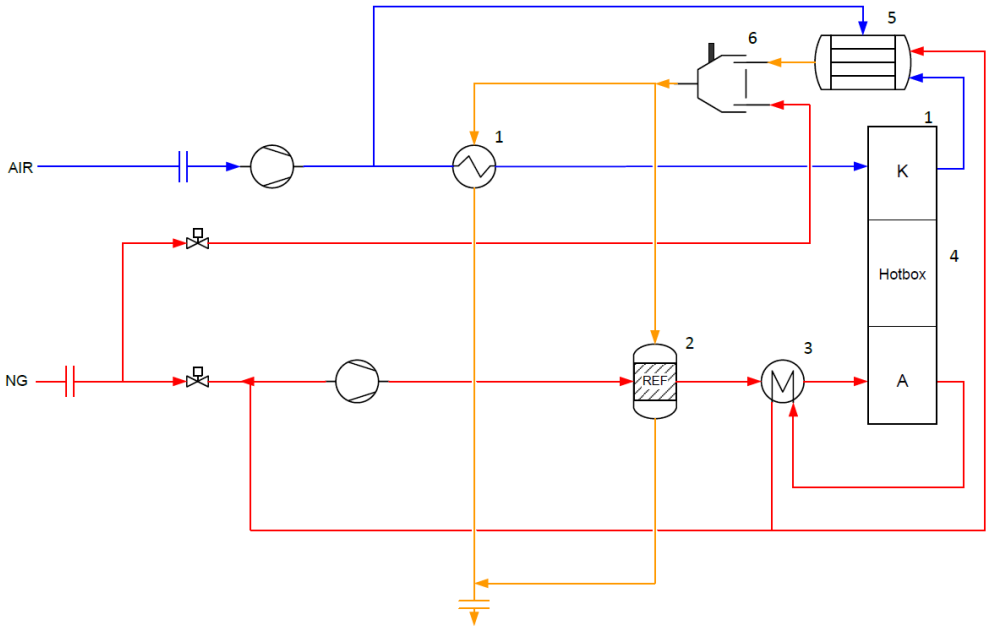

Figure 2.6 Flowsheet of the CHP - SOFC-System [16]

2.8.1 Preheating

In principal pre-reactions inside the preheater are initiated by the input of thermal energy to crack hydrocarbons. This process can also be described as pyrolysis or homogeneous gas phase reaction, which describes cracking between C and H-atoms and between C - atoms. Hereby the dissociation energy has to be overcome, for $C-C$ binding 345 kJ/mol, for $C-H$ binding 416 kJ/mol, for $C=C$ binding 615 kJ/mol and for $C\equiv C$ binding 811 kJ/mol. In case of a homogeneous gas-phase reaction cracking of $C-C$ is more likely than cracking of the $C-H$ bond. In the thesis of *Angerer,* several pyrolysis tests with LPG have been carried out, first with a numerical computer simulation program called *Chemkin* to compare published experimental data with temperatures up to 700°C. Furthermore, the numerical were evaluated in a plug flow reactor. As result, there is no development of unsaturated hydrocarbons in the temperate range of 350°C - 550°C and the formation of Acetylene (C_2H_2) can be excluded completely [15].

2.8.2 Heterogeneous catalysis

To achieve high conversion rates and low space time respectively, a solid catalyst is used for steam reforming. It lowers the energy barrier which the reactant must pass to form products. In general the catalyst speeds up the desired reaction rate without influencing the thermodynamic equilibrium or the end point of a reaction. Latter it is only governed by the thermodynamic.

The catalyst does not participate as a reactant and appears unchanged at the end of the reaction [16].

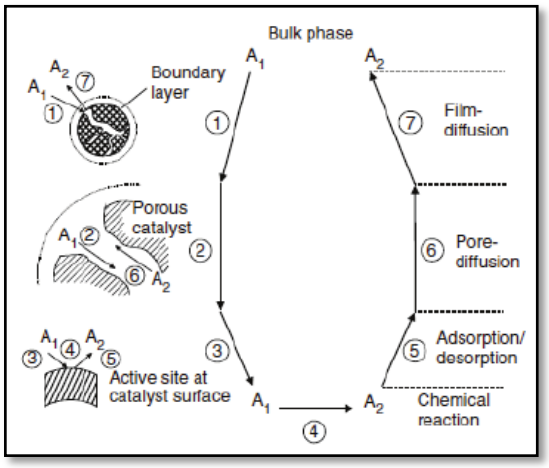

Figure 2.7: Individual steps of a simple, heterogeneous catalytic fluid-solid reaction carried out on a porous catalyst [17]

Heterogeneous catalysis can be described in seven sub steps [17].

1. the diffusion of the reactant from the boundary layer to the surface of the catalyst
2. diffusion of the reactant from the surface into the catalyst pores where the chemical transformation occurs
3. adsorption of reactant on the active catalyst surface
4. chemical reaction on the active side of the catalyst
5. desorption of the products
6. diffusion of the product from the inner pores to the surface
7. diffusion of the product from the boundary layer to the bulk

The heterogeneous reaction is until now not fully understood in its basic reaction mechanisms.

2.9 **Catalyst deactivation**

Catalyst deactivation is described as loss of activity and/or selectivity over time. In industrial processes the deactivation of catalysts is permanent and one of the most challenging problems. Deactivation can appear promptly or in several years but it always takes place [18].

Several types of catalyst deactivation are observed which are listed in table 2.4.

Table 2.4 Mechanisms of catalyst deactivation [18]

Mechanisms	Types	Brief description/definition
Poisoning	Chemical	Strong chemisorption of the kind on catalytic active surface, as a result blocking of sites for catalytic reaction
Fouling	Mechanical	Physical deposition of species from the fluid phase to the catalytic surface and in catalyst pores
Thermal degradation	Thermal	Thermally induced loss of catalytic surface area and support area
Vapour formation	Chemical	Reaction of gas molecules with catalyst, under formation of a volatile products
Attrition/crushing	Mechanical/Chemical	Mechanic-induced loss of internal surface area by crushing

The catalyst can be poisoned by impurities of the feed stream, for example by sulfurous components. The sulfur is chemisorped by the active species of Ni-reforming catalysts. The sulfur blocks the active species of the Ni because it has a stronger adsorption strength, relative to the other species. In the case of carbon formation active surface areas are covered or blocked which leads to blockage of catalyst pores or bursting of the particles [18].

High temperature reactions lead to thermally induced deactivation. Crystallites grow in the catalyst phase which leads to a loss of the catalytic activity. It can also cause the breakdown of support material and cause pore collapse. These processes can be described as „sintering". Additionally, the collapse leads to a reduction of the pore structure in carrier material or solid - solid reactions between the active catalytic phase and the carrier material, e.g. nickel aluminium

spinel. In the presence of oxygen, vapour formation leads to a deactivation of the catalyst by producing volatile compounds [18].

Sulfur poisoning in the case of SR of LPG is an important issue especially when a sulphur containing odorant is added to the gas. A further major challenge is to prevent carbon formation.

2.10 **Carbon deposition**

Carbon formation is one of the major problems in steam reforming of LPG on Ni based catalysts. Steam reforming is associated with high temperatures to produce hydrogen rich gas but it also supports the formation of carbon. These carbon formation appears in catalytic processes or even in side reactions where carbon monoxide is present. Both processes can lead to carbon deposition on the surface of the catalyst. In general, it can be suggested that two different types of carbon deposits „methynic" carbon C_α and „naphthenic" carbon C_β exist, depending on the formation conditions. Both carbons are formed under different conditions: C_α is more reactive than C_β. C_α is formed by oxidative dehydrogenation of propane. The second one ,C_β , is formed under conditions like dehydropolymerization of methyne groups on the surface of the catalyst [19].

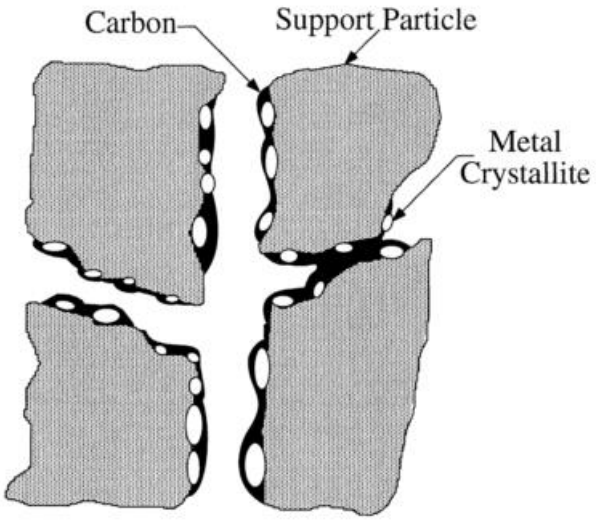

Figure 2.8 Model of crystallite encapsulation, fouling and plugging of catalyst material cause of carbon formation [18]

There are three different types:

- gum formation
- whiskers carbon
- pyrolytic carbon

The first one, gum formation, blocks the catalytic surface by polymerisation of C_nH_m radicals. That leads to progressive deactivation by low S/C-ratios, low temperature (< 500°C) and in presence of aromates.

Whisker carbon appears by the diffusion of C into Ni-crystallite. Carbon filaments grow on catalyst particles on top of the Ni. There is no deactivation of Ni-areas; it is more a bursting of the catalyst and a raise in pressure. Operation conditions with high temperatures (> 450°C) in presence of alkanes and aromates support whisker formation.

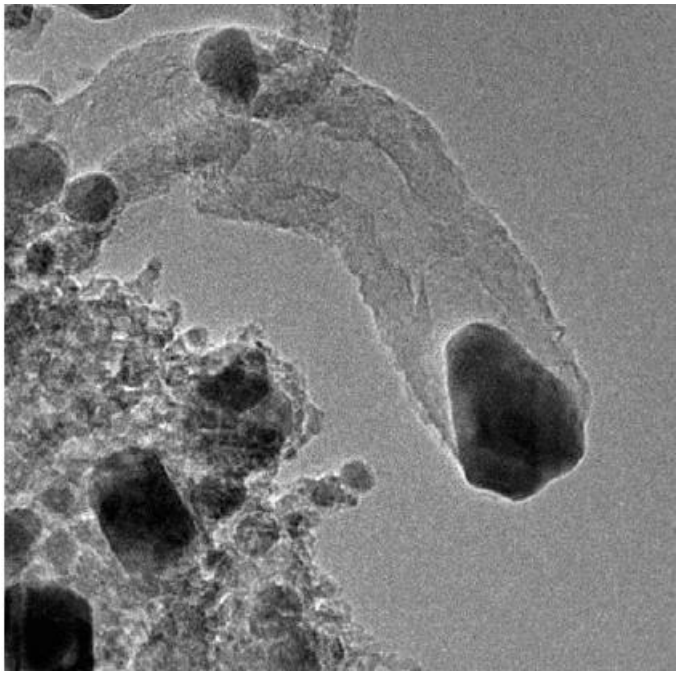

Figure 2.9 Whisker on Ni catalyst surface [20]

Pyrolytic carbon is formed by high temperature gas phase reactions with the formation of radicals. The radicals deposit as carbon on catalyst walls or encapsulate catalyst particles and the pressure rises. The development of pyrolytic

carbon is supported by high temperatures (> 600°C) and a long residence time. Also low S/C-ratios and alkanes support this process [20].

These depositions of carbon can be described by four chemical reactions [21], [22].

$$2CO \leftrightarrow C_{(s)} + CO_2 \quad \text{Equation 2.19}$$

$$CH_4 \leftrightarrow C_{(s)} + 2H_2 \quad \text{Equation 2.20}$$

$$CO + H_2 \leftrightarrow C_{(s)} + H_2O \quad \text{Equation 2.21}$$

$$C_nH_{2n+2} \rightarrow nC_{(s)} + (n+1)H_2 \quad \text{Equation 2.22}$$

The first three reactions are reversible reactions, therefore it is possible to remove carbon formation by gasification. Catalysts can be regenerated by mild oxidation substances such as H_2, CO_2 and H_2O.

There are two indicators for carbon formation and catalyst deactivation, increase in pressure and the rise of temperature. The rise of temperature can be an indication for catalyst deactivation; this behaviour can be explained by exothermic reaction (perhaps methanation) and by a decrease in the endothermic reaction e.g. SR [9].

To prevent Carbon formation it is necessary to run the catalyst in the optimum point of operation. Strategies to minimize carbon formation include oxidative or reductive regeneration or the development of coke resistant catalysts [21], [22].

2.11 **Critical Process Parameters**

This chapter provides an overview of key operating parameters and parameters to evaluate the performance of the catalyst. Especially the S/C-ratio, GHSV, influence the carbon formation and deactivation of a catalyst as can be read in chapter 2.10. These are the most important key parameters along with temperature [17].

Space time (τ)

Space time τ is defined as the time required to process one reactor volume of feed measured at specified conditions.

$$\tau = \frac{reactor\ volume}{volumetric\ feed\ rate} = \frac{V}{\dot{V}_o}$$ Equation 2.23

Space velocity (SV)

The SV is defined as number of reactor volumes of feed at specified conditions. The unit time is expressed by the reciprocal of the space time.

$$SV = \frac{1}{space\ time} = \frac{1}{\tau}$$ Equation 2.24

Gas hourly space velocity (GHSV)

The GHSV is defined as the ratio of the volumetric gas feed rate at standard conditions divided by the reactor volume.

$$GHSV = \frac{volumetric\ feed\ rate}{reactor\ volume} = \frac{\dot{V}_o}{V}$$ Equation 2.25

Steam to carbon ratio (S/C)

The S/C-ratio is a parameter to describe the proportion between steam and carbon. This parameter allows us to keep the proportion of hydrocarbon to steam constant by changing the GHSV to increase or decrease the space time.

$$SC = \frac{steam\ feed\ to\ the\ reactor}{C-atomes\ of\ hydrocarbon\ feed\ to\ the\ reeactor} = \frac{\dot{n}_{H_2}}{x* \dot{n}_{CxHy}}$$

Equation 2.26

Catalyst characterisation

Catalyst performance can be described usually by the three parameters conversion, selectivity and yield [17].

Conversion X_i

The fractional conversion describes how reactant A for example converts to something else. The conversion is generally based on the conversion of the amount of substance A_0 at t = 0 in mole, which is converted to product A at time t.

$$X_i = \frac{N_{A0} - N_A}{N_{A0}} \qquad \text{Equation 2.27}$$

Selectivity S

A catalyst does not change the thermodynamic equilibrium but it can support or suppress part reactions of a chemical reaction. It depends on the catalyst material or structure of a supported product type. On this basis it is possible to obtain different educts with the same products. The amount of product H_2 out of educt C_3H_8 is described by the selectivity:

$$S = \frac{Y}{X} = \frac{N_R - N_{R0}}{N_{A0} - N_A} \qquad \text{Equation 2.28}$$

Yield Y

To express the amount of how much educt A is converted to product R, describes the yield:

$$Y = \frac{N_R - N_{R0}}{N_{A0}} \qquad \text{Equation 2.29}$$

2.12 **Literature on steam reforming of LPG**

The following chapter provides an overview about papers and articles on steam reforming of LPG on nickel based catalyses. The purpose of this chapter is to find suitable process parameters for the experimental work and process parameters for the evaluation in the matlab model. Most of the literature refers to catalyst tests with different dopings of Ni catalysts to improve conversion rate, selectivity or coke resistance. Below, a summary of papers is listed.

In 2002 *K.Ahmed* published a paper about the reforming of LPG to produce methane, hydrogen and carbon oxidised syngas for internal reforming in a SOFC micro reactor. The micro reactor was scaled up to run a 500 h LPG reformer test. Several catalysts for performing tests under isothermal conditions were mentioned but it was not illustrated which catalysts were used. We do know, however that a commercially available catalyst in pellet form with a size of 4.7 mm was used for the micro reactor.

The aim of the tests was to evaluate the activity of LPG reforming under thermodynamically favourable conditions like temperatures between 350°C to 400°C and an S/C-ratio of 1.5 and 2. The micro reactor had a diameter of 5 cm and a volume of 500 cm^3, run by chemical pure propane. Experiments were carried out in a temperature range of 375°C – 400°C and a GHSV up to 21000 h^{-1}. As shown in figure 2.10, a test was performed in a temperature range of 350°C – 373°C, a S/C-ratio of 1.5 and SV of 5000 h^{-1}. The reformer feed rate was 3 l/min of LPG.

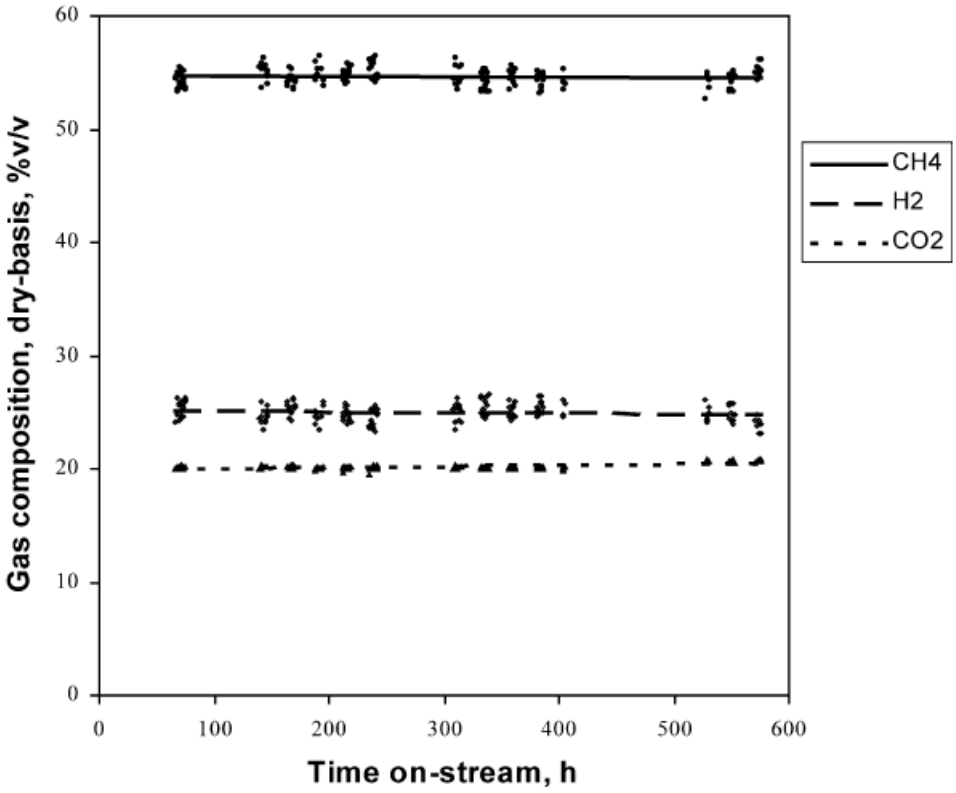

Figure 2.10 Long-term operation of a prototype LPG reformer [23]

As a result, the reformer gas on dry-basis contained 55 Vol - % methane (CH_4), 25 Vol - % hydrogen (H_2) and 20 Vol - % carbon dioxide (CO_2). In further tests the reformer was scaled up for a 500 h test and supplied enough hydrogen for a 5 kW system [23].

The following paper published in the international journal of hydrogen energy with the title *Development of highly effective supported nickel catalysts for pre-reforming of liquefied petroleum gas under low steam to carbon molar ratios* reports the pre-reforming of LPG in a Ni-CeO_2 catalyst. The advantage of this catalyst material lies in the low S/C-ratio that is less than 1. Also a comparison was made between a pure Ni catalyst and a Ni-CeO_2 catalyst. The author suggests S/C-ratio for pure Ni catalyst in a range between 2.5 - 4 and at temperatures range from 400°C – 500°C. The LPG was a mixture of 3,1 Vol - % ethane (C_2H_6), 84 Vol - % propane (C_3H_8), and 12,9 Vol - % butane (C_4H_{10}). Several tests were conducted with a several different CeO_2 dopings and it was proven that the catalyst could run with an S/C-ratio lower than 1 [24].

A further paper reports about a dual fuel system for SOFC using dimethyl ether and liquefied petroleum gas as a fuel. A commercial reforming catalyst based on Ni (FCR - 4, Süd-Chemie Catalyst) was used. First the reforming process was simulated by a computer program (HSC Chemistry for Windows 6.1, Outokumpu Research Oy, Finland) to evaluate the influence of reaction temperature on the S/C-ratio and on carbon formation. Additionally, the thermodynamic equilibrium was calculated with the help of a computer program. After reducing the catalyst at 700°C the fuel was fed to the catalyst at 550°C, the temperature was increased to 700°C and kept constant for 1 h at ambient pressure. The catalyst bed was supplied with propane at 20 sccm. The outlet gas was analysed by a micro GC. Carbon deposition was quantified by TPO. In the case of propane equilibrium calculations suggest a temperature of 550°C and S/C-ratio 1.8 [26].

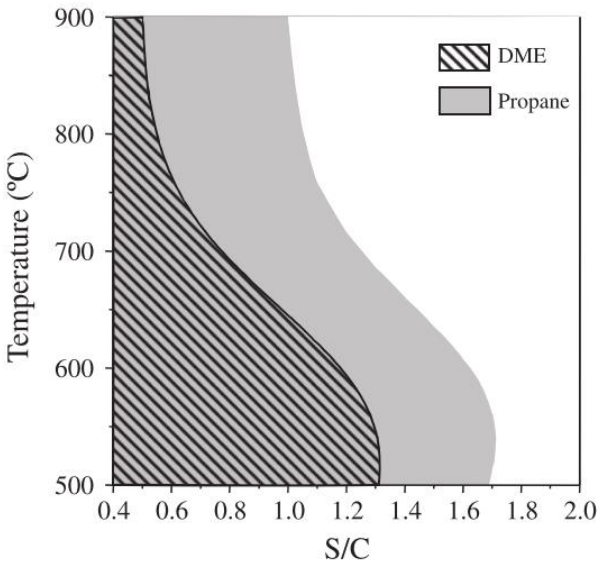

Figure 2.11 carbon deposition by steam reforming of propane and DME [26]

The actual tests were performed with an S/C-ratio of 3.5 and with a temperature of 550°C.Thus, almost all propane was converted and no carbon formation occurred. Compared to the equilibrium calculations in the temperature range between 500°C – 700°C there was a difference of ± 4% compared to the test result.

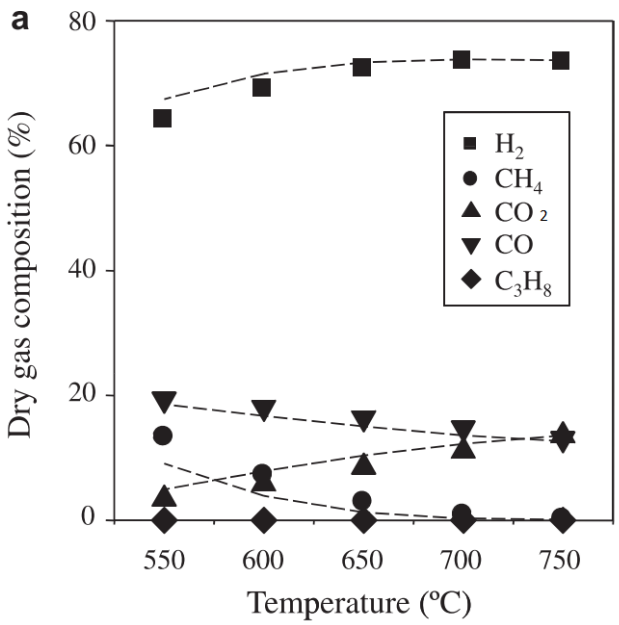

Figure 2.12 Dry gas composition of reformed propane gas at S/C-ratio 3.5 [26]

As a result, the computer program suggested an S/C-ratio of 1.8 for propane but the tests showed that an S/C-ratio above 3.5 was required for steam reforming of propane [26]. The transfer of the test result and of the critical process parameters to our test conditions was difficult because the LPG composition was not mentioned in the paper.

2.13 **Equilibrium calculation**

To pre-evaluate the key parameters in the literature, it was necessary to determine a range of parameters in a virtual reforming reactor in Simulink. Thus, for every S/C-ratio it was necessary to insert these parameters into the virtual reactor. The reactor can be described as isothermal. The outlet temperature at the end of the reactor was already predefined by previous diesel and methane tests. The outlet temperature was therefore taken for calculating the equilibrium. The reactor was based on a Gibbs reactor by minimising the Gibbs enthalpy $\Delta_R G$. Therefore, it was possible to draw an equilibrium curve for every S/C-ratio. Also a pre evaluation of the scope of the key parameters was already possible to prevent possible carbon formation. However, these results need to be treated carefully as mentioned in chapter 2.10. The carbon formation potential depends

primarily on the kinetics of the dissociation of respective hydrocarbons and less on thermodynamics. As a result, the computer simulation predicts a carbon formation although in reality no carbon formation accurse or vice versa. The only essential characteristic trait of the catalyst is whether it can repress or support the way of carbon formation [20].

3. Experimental Setup

This chapter „Experimental Setup" includes a description of all parts of the test rig and of its main component the reformer. Additionally, an explanation of the test procedure is given.

3.1 **Test rig**

The test rig as shown in figure 3.1 is made of up to the following components:

A – Gas supply

B – Sulfur trap

C – Evaporator

D – Diesel evaporator

E – Pre heater

F – Reformer

G – Heat exchanger

H – Gas analyser

Several tests have been conducted with different fuels such as diesel and methane with the test rig provided by AVL. For LPG feed several changes need to be made. The gas supply (A) for the test rig is obtained for commercially available propane gas bottles. A sulfur trap (B) is installed to clean the inlet gas from sulfur impurities, which in turn prevents a sulfur poisoning of the catalyst. After the blending of LPG and steam the gas is pre heated (E), the diesel evaporator (D) can be ignored as it had not been used in the tests. The inlet gas enteres reformer (F), which is filled with a Nickel catalyst and passes than the heat exchanger (G). To analyse the components of the outlet gas a gas analyser is connected to the outlet stream. The condensate storage vessel capture the condensate coming out of the outlet stream.

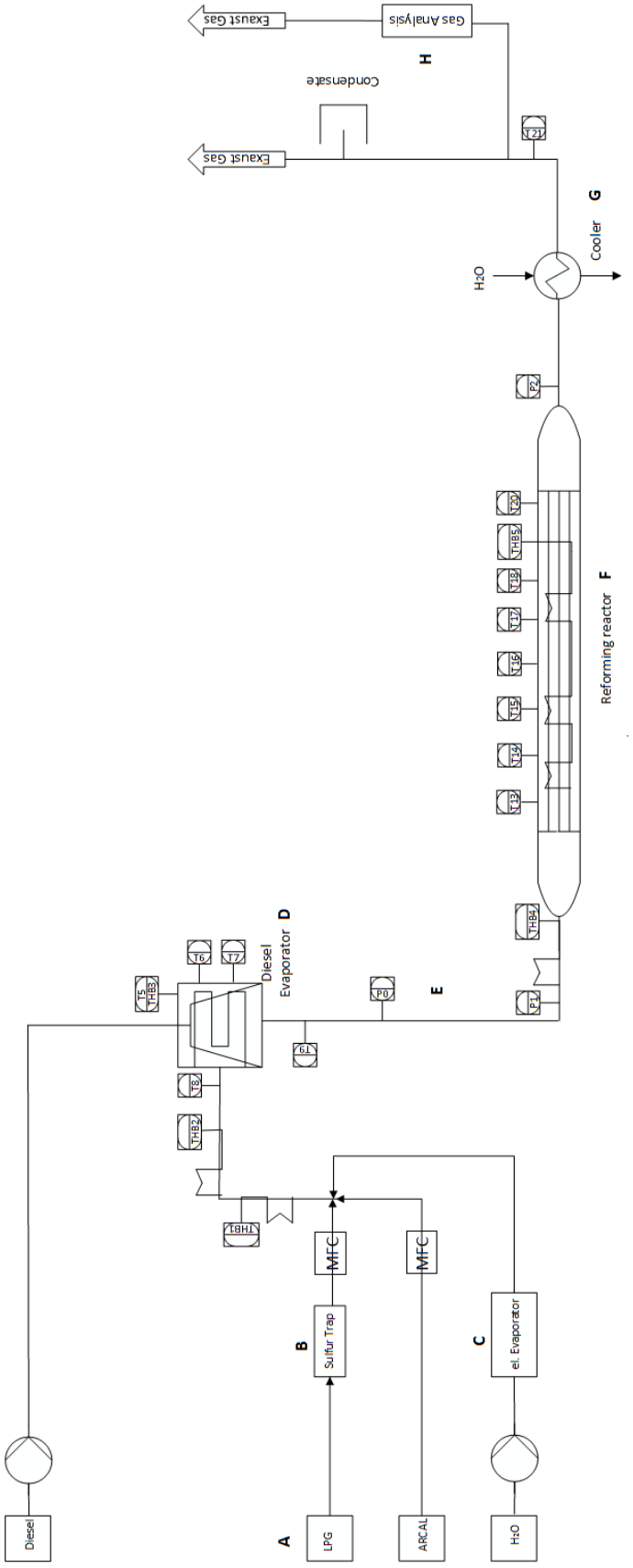

Figure 3.1 Flowsheet of the test rig

3.1.1 Gas supply

The test rig is supplied by two gases, forming gas *ARCAL,* a mixture of 95 Vol - % nitrogen (N_2), 5 Vol - % hydrogen (H_2) and LPG. The LPG bottles are stored and connected to a gas station as shown in figure 3.2. In this way, it is possible to connect three gas bottles in a row to ensure a permanent gas supply for several hours. Due to the separate connections (1) it is possible to exchange the gas bottles during the test by closing the valve (2) and by reopening it after changing the gas bottle. The pressure reducing valve (3) reduces the pressure from the inlet pressure 10 bar LPG bottle to 1,5 bar outlet pressure for the MFCs.

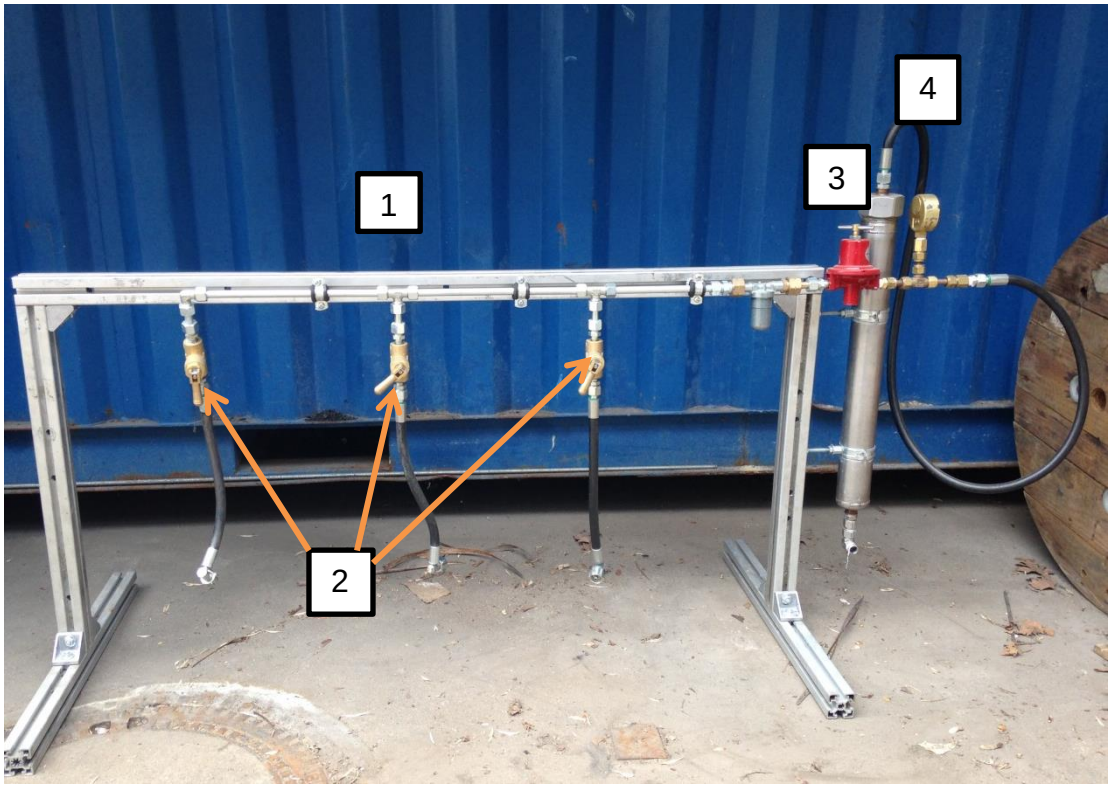

Figure 3.2 Gas station

As shown in figure 3.3 the sulfur trap (4) is mounted horizontally to the frame to prevent channel building in the adsorbent.

3.1.2 Sulfur Trap

Due to the specification of EN ÖNORM 590 LPG can contain a maximum amount of 50 ppm of sulfur, elemental sulfur and an odorant. Thus, the amount of sulfur needs to be reduced to 0,1 ppm [27] according to the manufacturers' specifications to prevent sulfur poisoning. In the outlet gas 5,34 ppm of sulfur were measured and 0,1 ppm after the sulfur trap.

A mixture of two different sulfur adsorbents was chosen and tested, both developed in cooperation with AVL and the manufacturer. In general the sulfur trap was over sized with a length of 55 cm and a diameter of 6 cm, just to make sure that no breakthrough of sulfur during the test time will occur. To harmonize the steam profile a layer of 3 cm gas spheres was filled on the top and the bottom of the sulfur trap. During the test time there was no breakthrough of sulfur monitored.

Figure 3.3 Sulfur Trap

3.1.3 Reformer Test Rig

The reformer test rig is shown in figure 3.4. The first two parts of the test rig are the extraction hood (1) and the exhaust gas pipe line (2). At the sampling point (3) an *ABB Advance Optima* and a *Micro GC Fusion Chromatogram* can be connected for analysing gas continuously and for taking gas samples with gas bags for the GC. For pre-heating (4) several heating coils are used, namely THB1, THB2 and THB3 to pre-heat the inlet gas to the desired temperature. The control system is connected to the switchboard and is controlled by *Lab-*

VIEW (5) for data logging. It is also monitoring temperature and pressure. After the reformer (10) the outlet gas needs to be cooled down, whereby water condenses, which is stored in a condensate storage vessel (6).The evaporator (7) is supplied by the water pump (8) *Stepdos 03 RC* with deionised water with a maximum flow rate of 30 ml/min. The water pump is connected to the water container (9) with a volume of 15 l. The reformer (10) represents the heart of the test rig and is filled with a Nickel catalyst, the specification of which can be seen in chapter 3.1.4.

On the reverse side of the test rig two MFCs *Bürkert 8626* are installed, one for the *ARCAL* and the second for LPG both gases are joined in a T-junction after the evaporator.

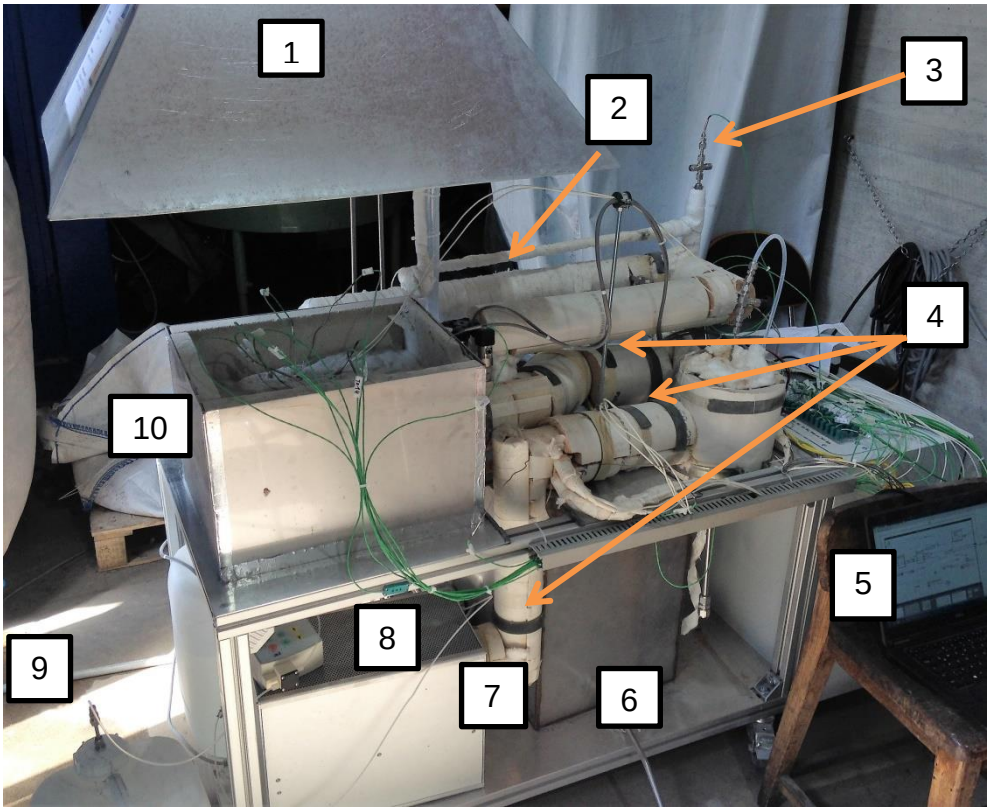

Figure 3.4 Reformer test rig

The reformer test rig is shown in figure 3.5 below. The two pressure sensors are the *APT 100* p1 inlet pressure sensor, and the p2 outlet pressure senor. They are both used to evaluate the pressure drop between the inlet and the outlet pressure in the reformer. The pressure difference was used to determine possi-

ble carbon formation inside the reactor. The heat exchanger (1) is used to cool down the outlet gas to prevent condensation in the sampling line.

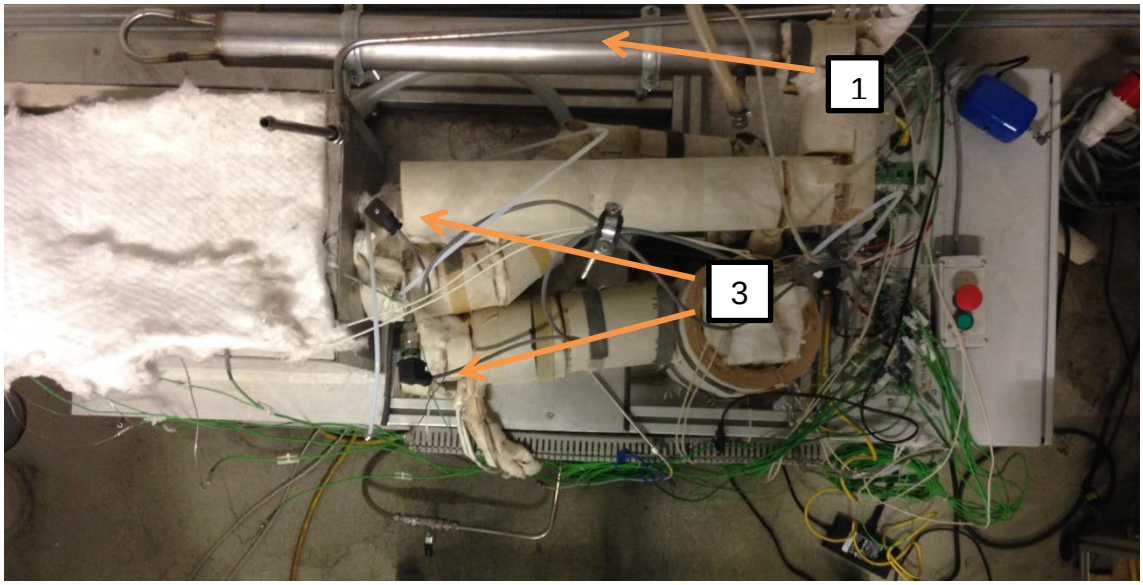

Figure 3.5 Reformer test rig top view

The control unit in figure 3.6 holds the whole switchboard from the National Instrument *CRIO-9067* and at the front side it contains five *EMKO* process controllers. The *EMKO* process controllers are PID controllers that are manually operated. On top of the control unit are five plugs for the heating coils, 21 plugs for the thermocouples and three plugs for the pressure sensors. Additionally, there are two *Bürkert 8626* mass flow controller plugs. The whole control unit was used for data logging in *LabVIEW*, for controlling the temperature, mass flow and pressure.

Figure 3.6 Control unit

3.1.4 Reformer

The reformer filled with the catalyst is the most critical element in this process. It needs to be active and selective for LPG. Furthermore it should be stable and resistant to poisoning. In figure 3.7 the reformer is shown as a metal tube in U-form and it is equipped with nine thermocouples T13 - T20 and wrapped with two heating coils, THB4 and THB5.

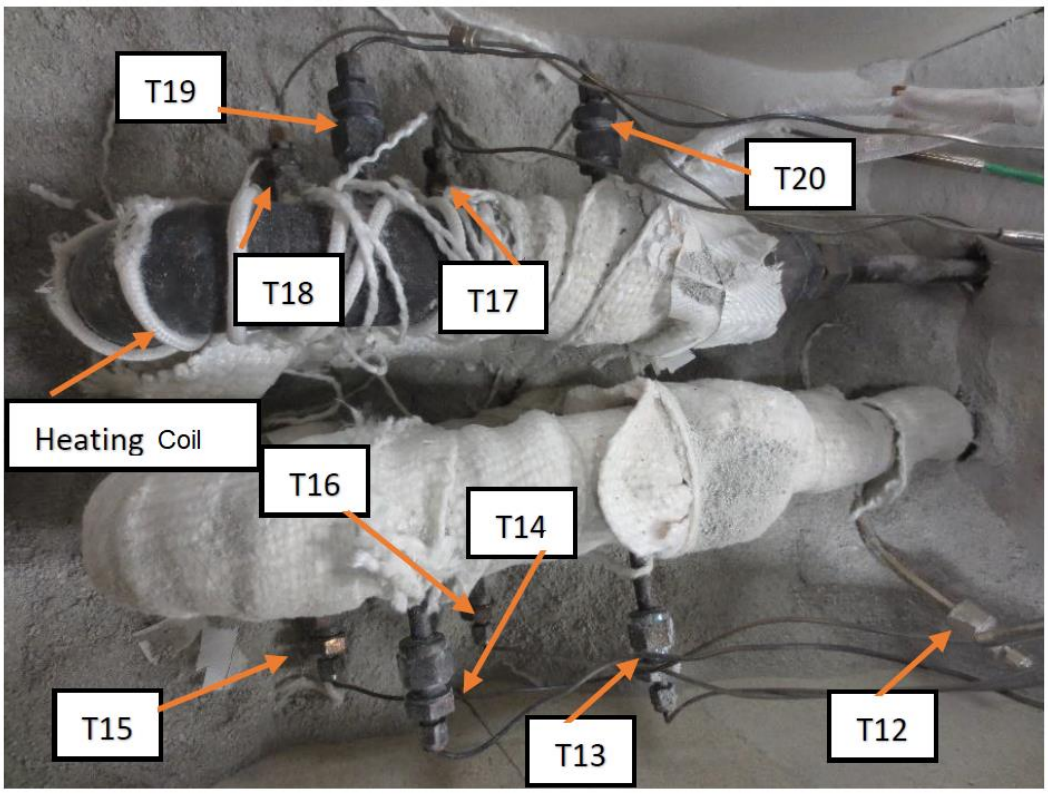

Figure 3.7: Reformer and thermocouples

The reformer in figure 3.7 is filled with a Ni based catalyst in form of pellets with sized 4.7 mm x 4.7 mm. The volume of the reformer is determined by the difference of the weight of the empty and filled catalyst being divided by the bulk density.

The bulk density was read from by the manual of the catalyst, to be 1,2 kg/dm³, whereby a volume of 0.75 dm^3 was calculated.

Figure 3.8 Catalyst

3.1.5 Gas analysis

The gas analyser took continuous samples at the sampling port with the help of the *ABB model AO2000* analyser with six different modules for CO_2, CO, CH_4, O_2 and H_2. In an excel file all data were logged every five seconds. A pump took an adjustable volume of gas and an upstream condenser prevented condensation in the gas analyser. The cooling equipment cooled down the inlet gas to 2°C, which was further analysed by the three detectors TCD, NDIR and an electrochemical cell. For analysing higher hydrocarbons and analysing gas in the medium test run a micro GC was used.

4. Experimental part

The following chapter describes all the procedures completed before the actual tests could start. First, the calibrations of the MFCs and the GC will be explained. Next, the reduction of the catalyst and the start-up procedure will be outlined, followed by the development of the test matrix based on the literature and the computer simulation. Finally, the test procedure will be explained in detail in a model case as can be seen in chapter 4.4.

4.1 **Calibration**

4.1.1 Calibration of the MFCs

The MFCs were calibrated to maintain the correct mass flow of LPG and to adjust the S/C-ratio. To calibrate the volume flow rate temperature and pressure were measured; in our case ambient pressure. The volume flow rate was measured with the bubble flowmeter *Glibrator-2* from the *Sensidyne* company. Thereby a gas cylinder was flooded with gas and by pressing a button a soap bubble was produced. The soap bubble moved upwards through the cylinder driven by the gas stream from the bottom to the top. By passing two light barriers, one on the bottom and the second on the top the time difference could be measured. This procedure was repeated several times in a series. With the following equation 4.1 the standard volume flow rate was calculated. The measured volume flow by *Gilibrator-2* is $\dot{V}_{Gil}$. The results and the data are available in the appendix.

$$\dot{V}_{norm} = \dot{V}_{Gil} * \frac{273{,}15}{T_u} * \frac{p_u}{1{,}01325} \qquad \text{Equation 4.1}$$

The second MFC for the reforming gas was already calibrated.

4.1.2 Calibration of the GC

Since LPG was never tested before at the CEET institute it was necessary to calibrate the GC for the LPG measurements. This was done with a calibration

gas from Linde with a purity of 99,999 Vol. - % of both gases. It was a mixture of 50 Vol. - % of propane and of 50 Vol. - % butane. With this high purity of gases it was possible to set a calibration point to analyse the main components of the used LPG in the original gas bottles. Furthermore it enabled us to detect possible inlet gas components in the outlet gas.

4.2 **Reduction of the catalyst and heat up procedure**

For the activation and heat up of the catalyst the inert gas *ARCAL* was used. The activation or heat up was performed in an *ARCAL* gas atmosphere and according to the manual.

1. The flowrate of *ARCAL* is set at 200 Nl/h and was constant until the end of the reduction procedure.

2. Heating up the catalyst at 100°C with a heating rate of 50°C per h.

3. Further heating-up to 120°C with a heating rate of 15°C per h until the last thermocouple T20 reach 120°C and then keeping it steady for 1 h.

4. The heating rate can now be increased again to 50°C per h until 350°C; from now on no interruptions of *ARCAL* gas should appear.

5. Further heating with a heating rate of 50°C per h until the final temperature is reached with THB1 = 350°C, THB2 = 450°C, THB3 = 510°C and THB4 = 545°C and THB5 = 545°C. The temperature needed to be held constant for 10 h.

This procedure was always performed at every start up. The activation was only once as performed because the catalyst was never changed.

4.3 **Test matrix**

Before the tests started the key parameters were evaluated on the basis of literature data and with the help of a *Simulink* computer program. Based on this research results, a test matrix was developed and a carbon free area was defined. Furthermore, boundary conditions were pre-defined, and the temperature

was set at 550°C in the reformer, as the temperature range should be comparable to previous methane and diesel tests. Additionally, the content of CH_4 is limited to 15 Vol. - % in the outlet gas because of the type of fuel cell, which could not deal with higher contents of CH_4. The pressure can be described as ambient pressure 1013 hPa.

Table 4.1. Test series

Reformer temperature and pressure: THB4 = 545°C, THB5 = 545°C, p = 1013 [hPa] test duration = 2 [h]				
GHSV [1/h]				
1. Test series SC = 3 = const.	1500	2000	2500	3000
SC [-]				
2. Test series GHSV = 1500 [1/h] = const.	1,5	2	2,5	3

4.4 **Test procedure**

The first test series is aimed to prove that LPG reforming is possible with the catalyst and it was additionally aimed to find out how to operate the test rig. The first test was carried out with an S/C-ratio of 3; this S/C-ratio was chosen because it was almost confirmed that no carbon formation would accrue for a test duration of at least 2 h. Also this ratio was suitable for a first test experience with the test rig.

Respectively one test will be explained in detail.

The first test was done with an S/C-ratio of 3 and a GHSV of 1500 1/h. These figures can be described as being representative of moderate conditions for the catalyst. At the beginning there was the start up process, which is mentioned in chapter 4.2. After the start-up process the temperature was stable at 550°C in the reformer and continuously flushed with *ARCAL* (300 Nl/h) to have a reduced atmosphere. The amount of LPG and water was calculated by an excel program. It provided the amount of LPG per Nl/h, the amount of water in ml/min to meet the desired S/C-ratio and GHSV. The program supplied all the necessary information needed for the *LabView* program. With the *LabView* program in figure 3.4 installed at the control system it was possible to operate the test rig.
Also, the GA was connected to the gas sampling point that can be seen in figure 3.4. For later tests the GA wasn't available anymore so it was switched to gas sampling bags, which were analysed by a micro GC.
Before the test could start safety precautions needed to be taken. The ventilator of the extraction hood as well as the CO_2 sensor and the C_3H_8 / C_4H_{10} sensors needed to be switched on. The C_3H_8 / C_4H_{10} sensors were placed on the ground because these gases are heavier than air. As a result, the gas will be first detected on the ground.
After the safety check the actual test could start. First, the maximum temperature and pressure difference needed to be set in the LabView program in order to have a safety shut down triggered in case of overheating or sudden pressure rise in the system.

Then the amount of LPG was set by the MFC and the amount of water was set manually for the water pump. The change from inert gas to LPG could be started. First the water pump was switched on with the right amount of water and then it was held constant for about 5 minutes. That resulted in a peak pressure and temperature as can be seen in the diagram on the bottom in figure 4.3. Furthermore, the temperatures T6, T7 and T8 in the pre-heating zone as well as temperatures in the reformer T13 - T20 started to move. After a couple of minutes the temperature, pressures and concentrations measured in the GA stabilised themselves.

Then the *ARCAL* was switched off and the MFC of LPG was turned on, which lead to a further pick in the pressure diagram in some cases. But pressure and concentration stabilised themselves very quickly. As an immediate effect temperatures in the reformer T13 - T20 decreased due to the strong endothermal behaviour of the chemical reaction. At the moment, the reforming test started and was held constant for 2 h of test duration.

After the test time the LPG supply was switched off and the *ARCAL* supply with 300 Nl/h was turned on again to hold the catalyst in reducing atmosphere. The temperature increased immediately to its initial temperatures and the water pump was set to 10 ml/h to wash the reformer. It was washed until no CO_2 was detected anymore, represented in the blue frame graphically in figure 4.1.

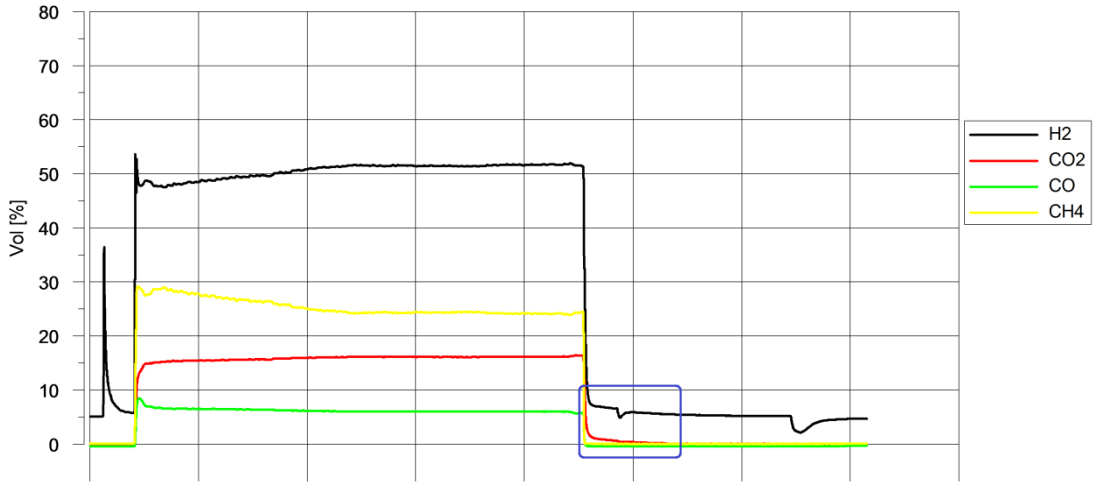

Figure 4.1 CO_2 reduction by washing the catalyst

The diagram below figure 4.3 can be split into four different diagrams. The first one shows the concentrations in Vol. - % of the measured components in the GA over time.

The second diagram represents the temperatures in the reformer and the third one the temperature in the pre-heating zone over time. The last one is the pressure diagram of the inlet- and outlet pressure. The most important pressure is $p_{1;}$ in some cases this pressure raises, which is an indicator for carbon formation. The $\Delta p_{relative}$ [mbar] table 4.2 is calculated by the difference of out let pressure p_1 and inlet pressure p_1 represented in an example in figure 4.2.

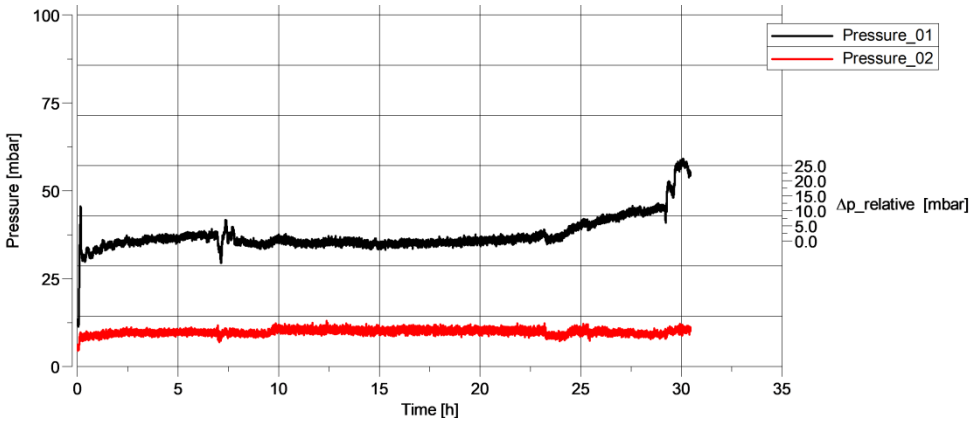

Figure 4.2 $\Delta p_{relative}\ [mbar] = p_{1\ out} - p_{1\ in}$

The pressure difference of p_1 to p_2 could not be used as an indicator of possible carbon formation because it depends on GHSV. This is illustrated in figure 8.6.

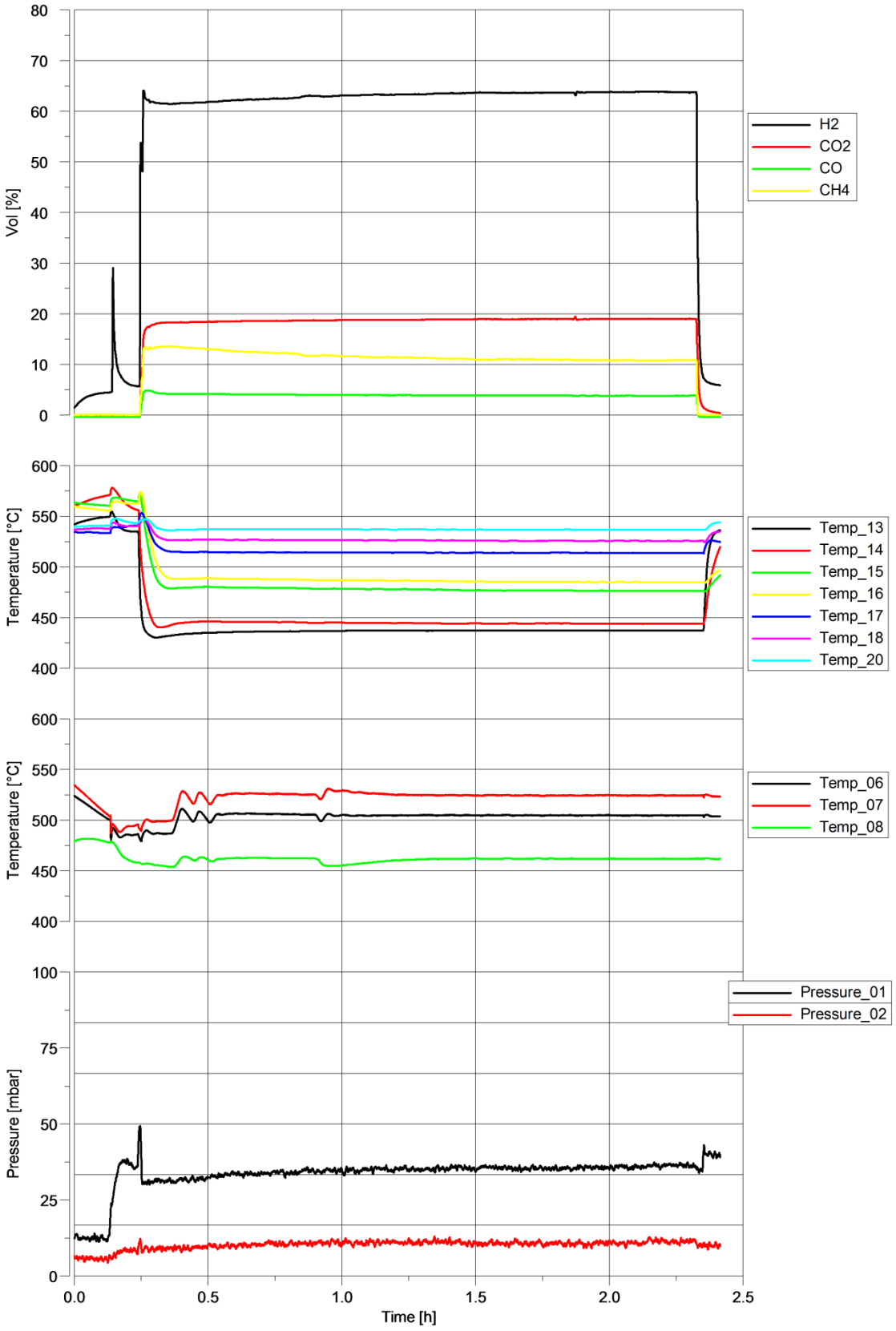

Figure 4.3 Temperature and pressure diagram: S/C 3; GHSV 1500;

$$\dot{V}_{LPG} = 111\ [Nl/h];\ \dot{V}_{H_2O} = 1014\ [Nl/h];\ T_{ref} = 550\ °C$$

The measured outlet volume ratios (dotted line) were compared to the theoretical equilibrium curve calculated by *matlab* (full line) as illustrated in the diagram figure 4.4. The green bar highlights the temperature range, which intercepts with the equilibrium curve and the volume ratios measured by the GA. In that case (shown in figure 4.4) the equilibrium curve is in accordance with the requirements, which are in the temperature range of the reformer.

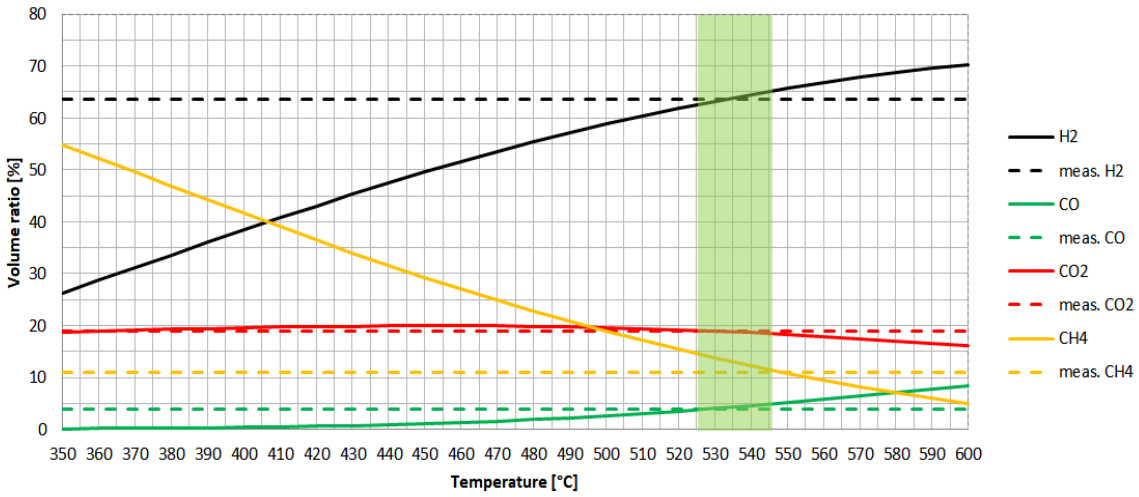

Figure 4.4 Equilibrium curve measured volume ratio: S/C 3; GHSV 1500 [1/h]

The table below shows the deviation between the calculated equilibrium by matlab and the measured Vol. - % from the GA or later from the GC.

Table 4.2 Deviation of volume ratio to equilibrium at T = 545°C calculated by matlab and relative pressure difference

Component	Volume ratio [%]	Equilibrium at T 545°C [%]	Deviation [%]
H_2	64	64	0
CO	4	5	20
CO_2	19	19	0
CH_4	11	12	8
$\Delta p_{relative}$ $[mbar]$		0	

5. Results

The following chapter summarises the results of all test series.

5.1 1. Test series

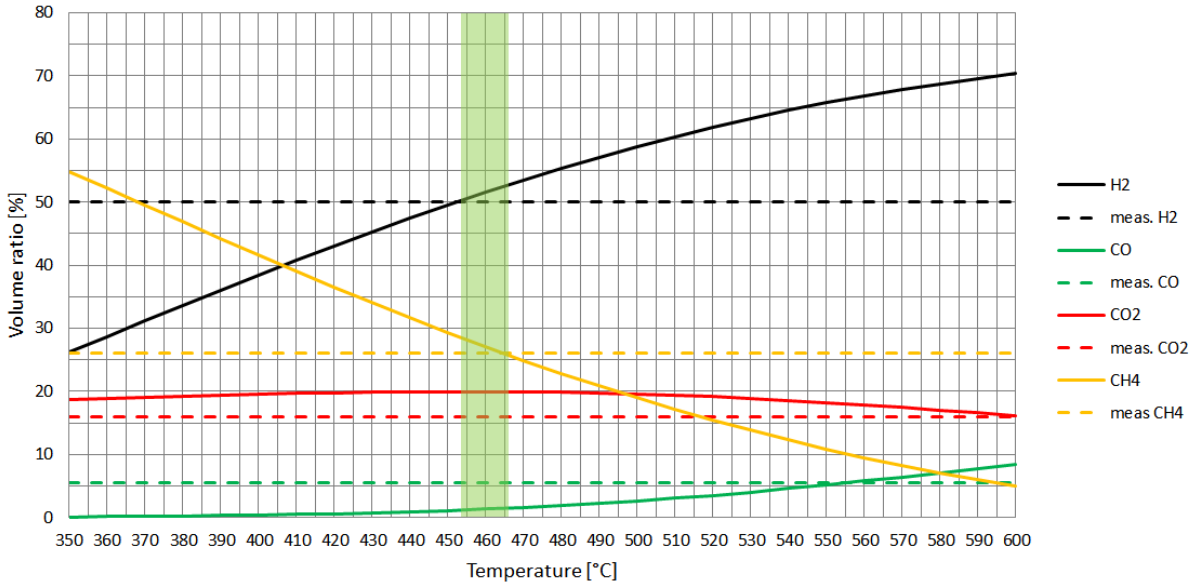

Figure 5.1 Equilibrium curve measured volume ratio: S/C 3; GHSV 2000 [1/h]

Table 5.1 Deviation of volume ratio to equilibrium at T = 545°C calculated by matlab and relative pressure difference

Component	Volume ratio [%]	Equilibrium at T 545°C [%]	Deviation [%]
H_2O	50	64	22
CO	6	5	20
CO_2	16	19	16
CH_4	26	12	117
$\Delta p_{relative}$ $[mbar]$		0	

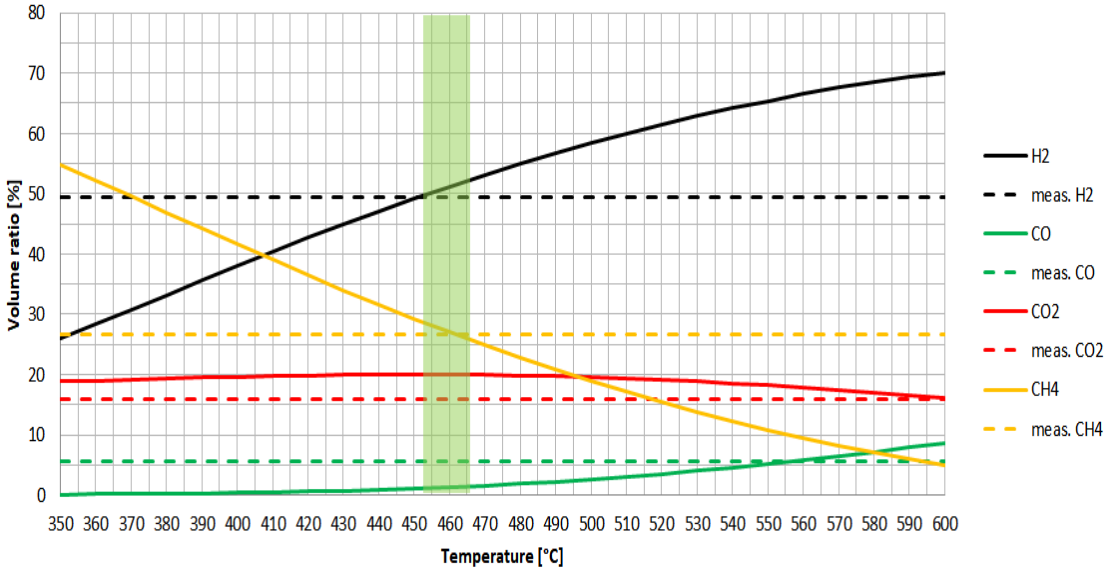

Figure 5.2 Equilibrium curve measured volume ratio: S/C 3; GHSV 2500 [1/h]

Table 5.2 Deviation of volume ratio to equilibrium at T = 545°C calculated by matlab and relative pressure difference

Component	Volume ratio [%]	Equilibrium at T 545°C [%]	Deviation [%]
H_2	50	64	22
CO	6	5	20
CO_2	16	19	16
CH_4	27	12	150
$\Delta p_{relative}\ [mbar]$		5	

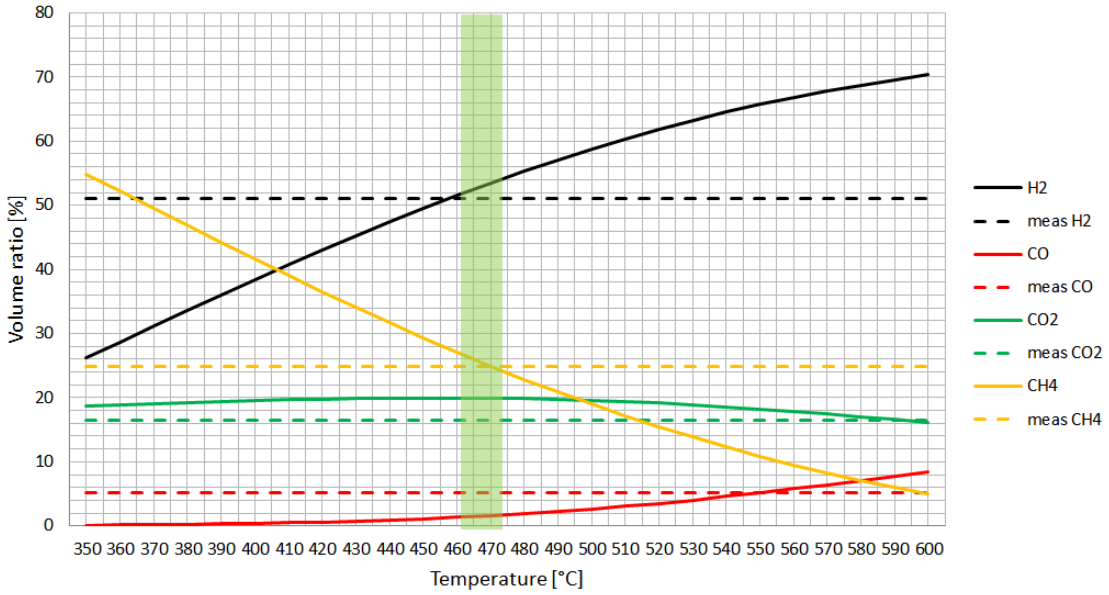

Figure 5.3 Equilibrium curve measured volume ratio: S/C 3; GHSV 3000 [1/h]

Table 5.3 Deviation of volume ratio to equilibrium at T = 545°C calculated by matlab and relative pressure difference

Component	Volume ratio [%]	Equilibrium at T 545°C [%]	Deviation [%]
H_2	51	64	20
CO	5	5	0
CO_2	17	19	11
CH_4	25	12	108
C_2H_4		0	
C_2H_2		0	
C_3H_8		0	
C_3H_4		0	
C_4H_{10}		0	
C_6H_{14}		0	
C_7H_{16}		0	
$\Delta p_{relative}$ $[mbar]$		5	

5.2 **Summary**

The first test series was carried out with a constant S/C-ratio of 3 and the GHSV was continuously increased from 1500 1/h – 3000 1/h. The temperatures were set at THB4 = 545°C, THB5 = 545°C. The first test was done with an S/C = 3 and a GHSV of 1500 1/h. It was shown that the catalyst works with LPG under these test conditions. The calculated equilibrium curve and the measured volume ratios of the components are intercepting the favourable temperature range of 525°C - 545°C, which represents the catalyst temperature. In further

tests the GHSV was increased and it was shown that with higher GHSV the temperature range decreases further in the range between 455°C - 475°C. A possible explanation would be a stronger endothermic reaction. As a result the volume ratio of H_2 declines and the volume ratio of CH_4 rises, which was already mentioned in literature. Other components such as CO and CO_2 remained almost constant. Finally, the deviation of calculated and measure volume ratio increases significantly with higher GHSVs. The relative pressure differences between the inlet pressure and the outlet pressure of p1 have not been raised.

5.3 **2. Test series**

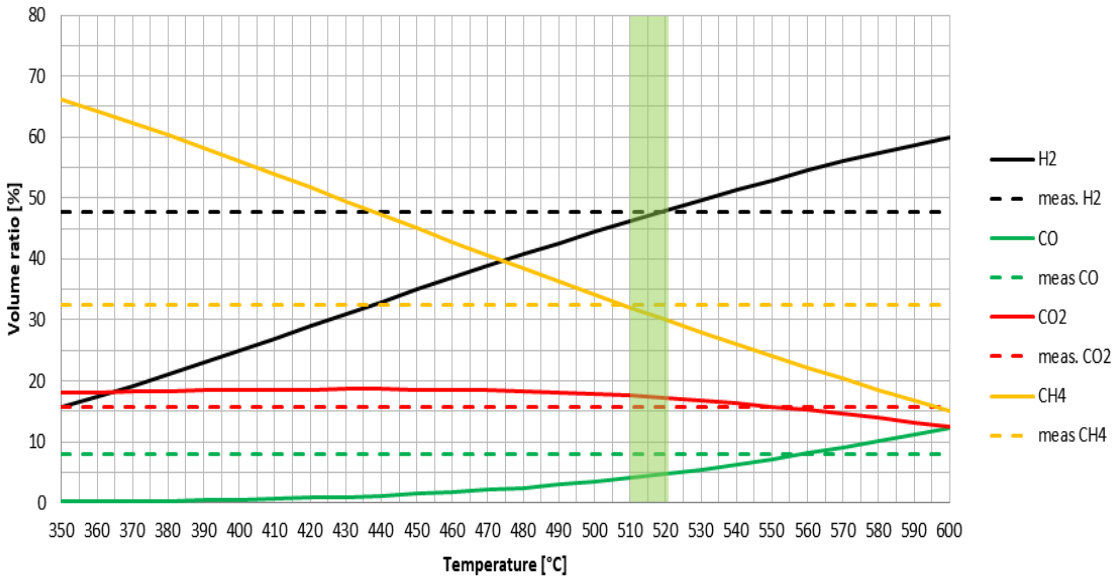

Figure 5.4 Equilibrium curve measured volume ratio: S/C 1, 5; GHSV 1500 [1/h]

Table 5.4 Deviation of volume ratio to equilibrium at T = 545°C calculated by matlab and relative pressure difference

Component	Volume ratio [%]	Equilibrium at T 545°C [%]	Deviation [%]
H_2	48	51	6
CO	8	6	33
CO_2	16	16	0
CH_4	32	26	23
C_2H_4		0	
C_2H_2		0	
C_3H_8		0	
C_3H_4		0	
C_4H_{10}		0	
C_6H_{14}		0	
C_7H_{16}		0	
$\Delta p_{relative}\ [mbar]$		0	

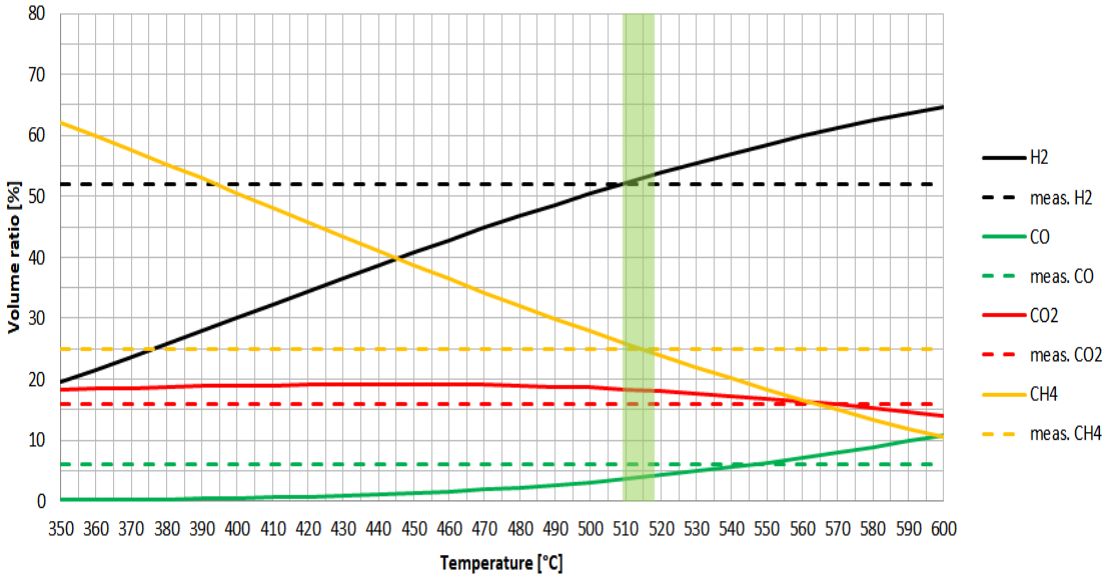

Figure 5.5 Equilibrium curve measured volume ratio: S/C 2; GHSV 1500 [1/h]

Table 5.5 Deviation of volume ratio to equilibrium at T = 545°C calculated by matlab and relative pressure difference

Component	Volume ratio [%]	Equilibrium at T 545°C [%]	Deviation [%]
H_2	52	57	9
CO	6	6	0
CO_2	16	17	6
CH_4	25	20	25
$\Delta p_{relative}\ [mbar]$		12	

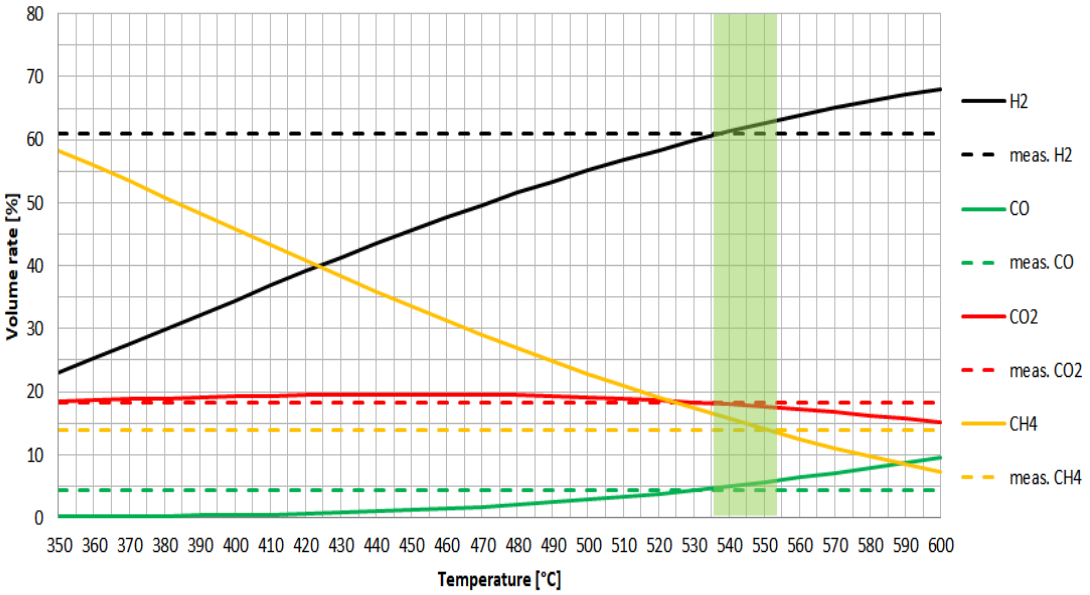

Figure 5.6 Equilibrium curve measured volume ratio: S/C 2, 5; GHSV 1500 [1/h]

Table 5.6 Deviation of volume ratio to equilibrium at T = 545°C calculated by matlab and relative pressure difference

Component	Volume ratio [%]	Equilibrium at T 545°C [%]	Deviation [%]
H_2	61	61	0
CO	4,	5	20
CO_2	16	18	11
CH_4	14	16	13
$\Delta p_{relative}\ [mbar]$		0	

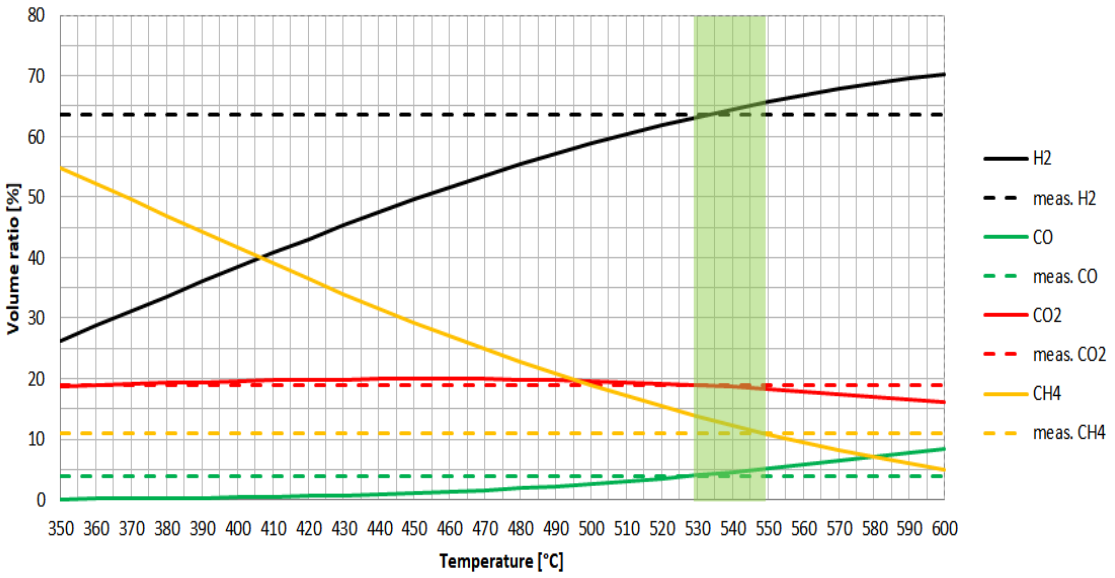

Figure 5.7 Equilibrium curve measured volume ratio: S/C 3; GHSV 1500 [1/h]

Table 5.7 Deviation of volume ratio to equilibrium at T = 545°C calculated by matlab and relative pressure difference

Component	Volume ratio [%]	Equilibrium at T 545°C [%]	Deviation [%]
H_2	64	64	0
CO	4	5	20
CO_2	19	19	0
CH_4	11	12	8
$\Delta p_{relative}$ $[mbar]$		0	

5.4 **Summary**

The first test with an S/C = 3 and a GHSV of 1500 met the requirement very well, thus it proved reasonable to proceed with the 2nd teste series. The GHSV of 1500 1/h was set constant and the S/C-ratio was continuously lowered from 3 to 1,5. Temperature and pressure were set again accordingly to the previous conditions. In the first two tests the calculated equilibrium curve and the measured volume ratios intercepting the desired temperature range between 530°C - 550°C, which is an indicator that the equilibrium was hit correctly. In later tests with S/C-ratios of 2 and 1,5 the temperature range decreased to 510°C - 520°C. That also had an effect on the outlet gas mixture; volume ratio changed from high content of H_2 e.g. 61 Vol - % to 48 Vol - % by an S/C-ratio of 1,5. The reverse effect could be seen with CH_4 at low S/C-ratio; the content of CH_4 increased and with high S/C-ratio the content decreased due to the WGS reaction. It is, that lower S/C-ratio leads to higher CO concentration in the outlet gas. The CO_2 concentration remains constant over the different S/C-ratios. The deviation of calculated and measured volume ratio is also constant over the measured S/C-ratio. Furthermore, there is no increase in pressure difference between the inlet and the outlet pressure of p_1. This test series has shown how the S/C-ratio influences the volume ratios, which in important for meeting the boundary conditions of the SOFC.

5.5 **Extended test series**

Table 5.8 Extended test series

Reformer temperature and pressure: THB4 = 545°C, THB5 = 545°C, p = 1013 [hPa] test duration = 2 [h]			
GHSV [1/h]			
SC = 2,5 = const.	2000	2500	3000

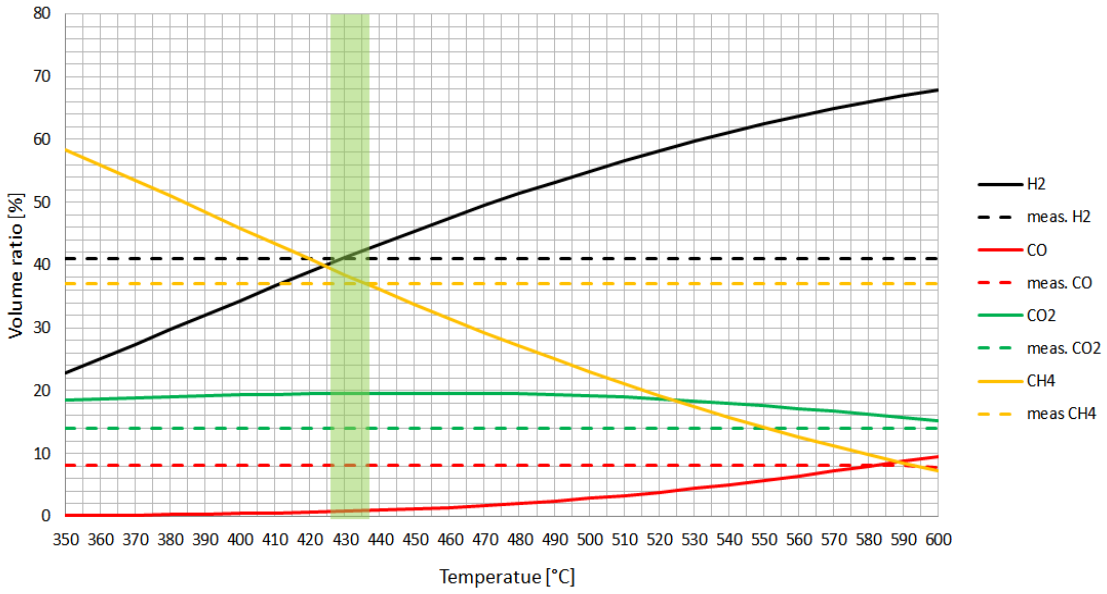

Figure 5.8 Equilibrium curve measured volume ratio: S/C 2,5; GHSV 2000 [1/h]

Table 5.9 Deviation of volume ratio to equilibrium at T = 545°C calculated by matlab and relative pressure difference

Component	Volume ratio [%]	Equilibrium at T 545°C [%]	Deviation [%]
H_2	41	61	33
CO	8	5	60
CO_2	14	18	22
CH_4	37	16	131
C_2H_4		0	
C_2H_2		0	
C_3H_8		0	
C_3H_4		0	
C_4H_{10}		0	
C_6H_{14}		0	
C_7H_{16}		0	
$\Delta p_{relative}\ [mbar]$		63	

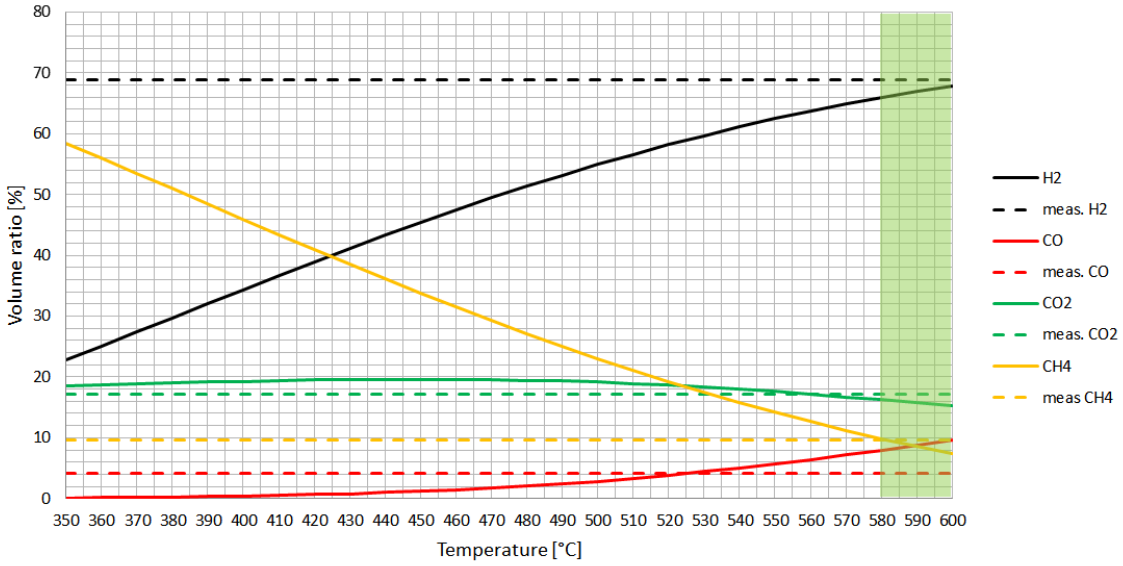

Figure 5.9 Equilibrium curve measured volume ratio: S/C 2,5; GHSV 2500 [1/h]

Table 5.10 Deviation of volume ratio to equilibrium at T = 545°C calculated by matlab and relative pressure difference

Component	Volume ratio [%]	Equilibrium at T 545°C [%]	Deviation [%]
H_2	59	61	3
CO	4	5	20
CO_2	17	18	6
CH_4	10	16	40
C_2H_4		0	
C_2H_2		0	
C_3H_8		0	
C_3H_4		0	
C_4H_{10}		0	
C_6H_{14}		0	
C_7H_{16}		0	
$\Delta p_{relative}$ $[mbar]$		112	

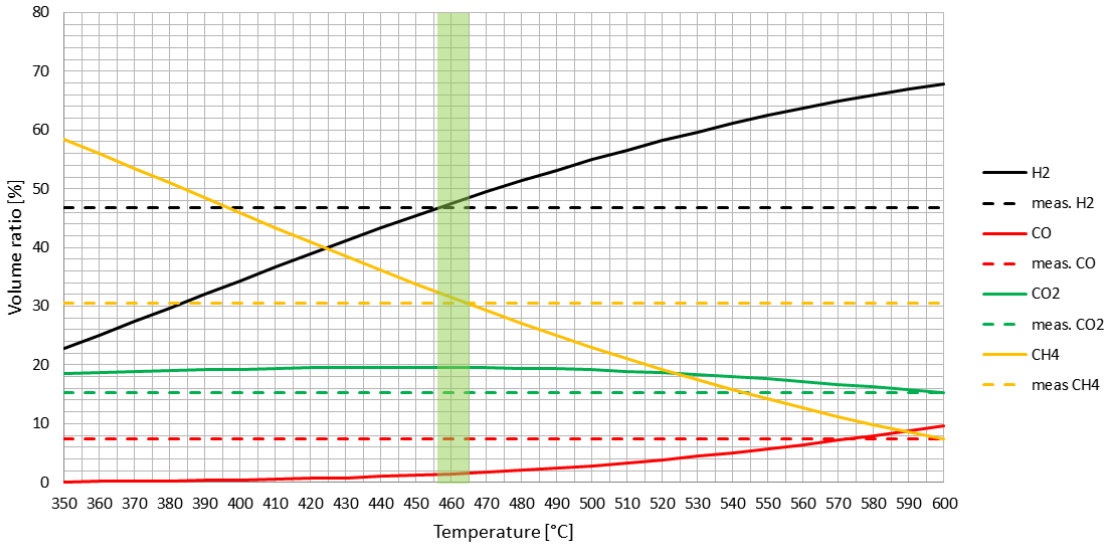

Figure 5.10 Equilibrium curve measured volume ratio: S/C 2,5; GHSV 3000 [1/h]

Table 5.11 Deviation of volume ratio to equilibrium at T = 545°C calculated by matlab and relative pressure difference

Component	Volume ratio [%]	Equilibrium at T 545°C [%]	Deviation [%]
H_2	47	61	23
CO	7	5	40
CO_2	15	18	17
CH_4	30	16	90
C_2H_4		0	
C_2H_2		0	
C_3H_8		0	
C_3H_4		0	
C_4H_{10}		0	
C_6H_{14}		0	
C_7H_{16}		0	
$\Delta p_{relative}$ $[mbar]$		62	

5.6 **Summary**

After the first two test series an extended test series was carried out with a constant S/C-ratio and a continuous increase of GHSV, since the first test series with a S/C-ratio of 2,5 and a GHSV of 1500 1/h had met the requirements of a low S/C-ratio and small deviation. The test conditions were picked up again and were further investigated. The first noticeable aspect is that none of the tests intercepting the equilibrium curve in the measured temperature range of the catalyst. Also the deviation of all the conducted tests is significantly higher compared to the earlier tests. Additionally, the relative pressure rises after a short period of time, roughly after 1 h or even earlier, as can be seen figure 9.9; figure 9.10; figure 9.11. Temperature T 13 rises at the same time as the pressure rises in the first test of the extended test series, cf. figure 5.8. In the second figure 9.10 and third figure 9.11 the tests show that T13 is even higher than T 14. In the first and the third test the volume ratio of H_2 compared to the second test was higher. With CH_4, however, it is the other way around. As a result, all three testes had a strong rise in pressure, being significantly higher than in all of the previous before.

5.7 **Medium Test Run 30 h**

After three test series it was decided that an S/C-ratio of 2,5 and a GHSV of 1500 1/h would constitute the most suitable test condition for the medium test run . The previous tests have shown, the temperature range was very close to the operating conditions of the reformer. Also the deviations between the calculated equilibrium and the measured volume ratios were quite small. There was no pressure rise during the 2 h test duration. Furthermore, the methane content was in the desired range below 15 Vol - %.

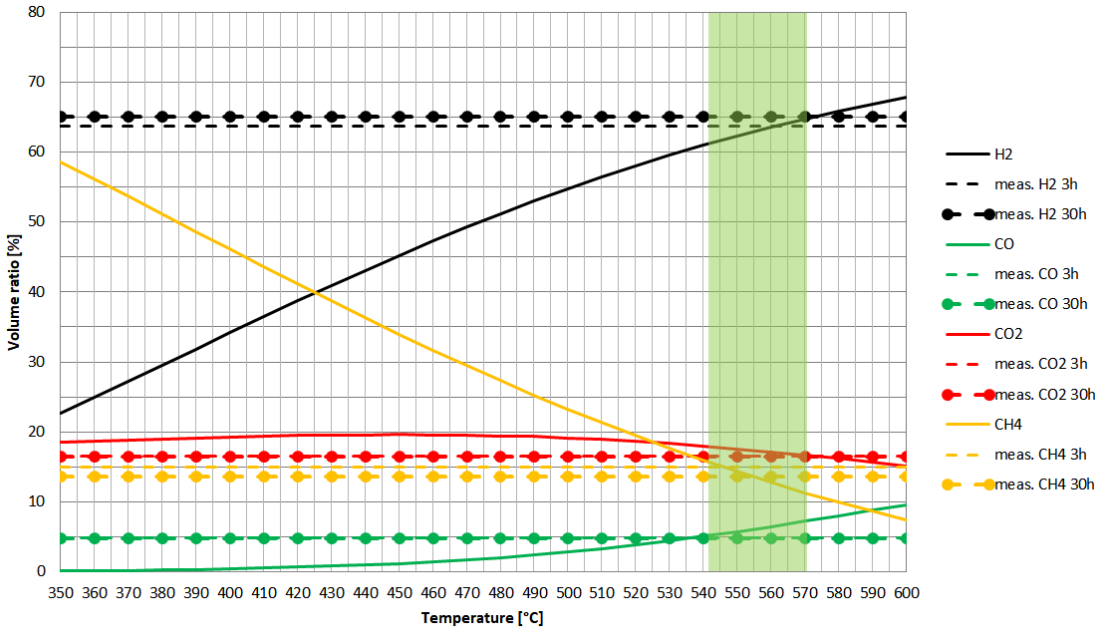

Figure 5.11 Equilibrium curve measured volume ratio: S/C 2,5; GHSV 1500 [1/h]

Table 5.12 Deviation of volume ratio to equilibrium at T = 545°C calculated by matlab and relative pressure difference

Component	Volume ratio [%] 5h	Volume ratio [%] 30h	Equilibrium at T 545°C	Deviation [%]
H_2	63	65	61	5
CO	5	4	5	10
CO_2	17	17	18	0
CH_4	15	14	16	9
C_2H_4	0			
C_2H_2	0			
C_3H_8	0			
C_3H_4	0			
C_4H_{10}	0			
C_6H_{14}	0			
C_7H_{16}	0			
$\Delta p_{relative}\ [mbar]$	25			

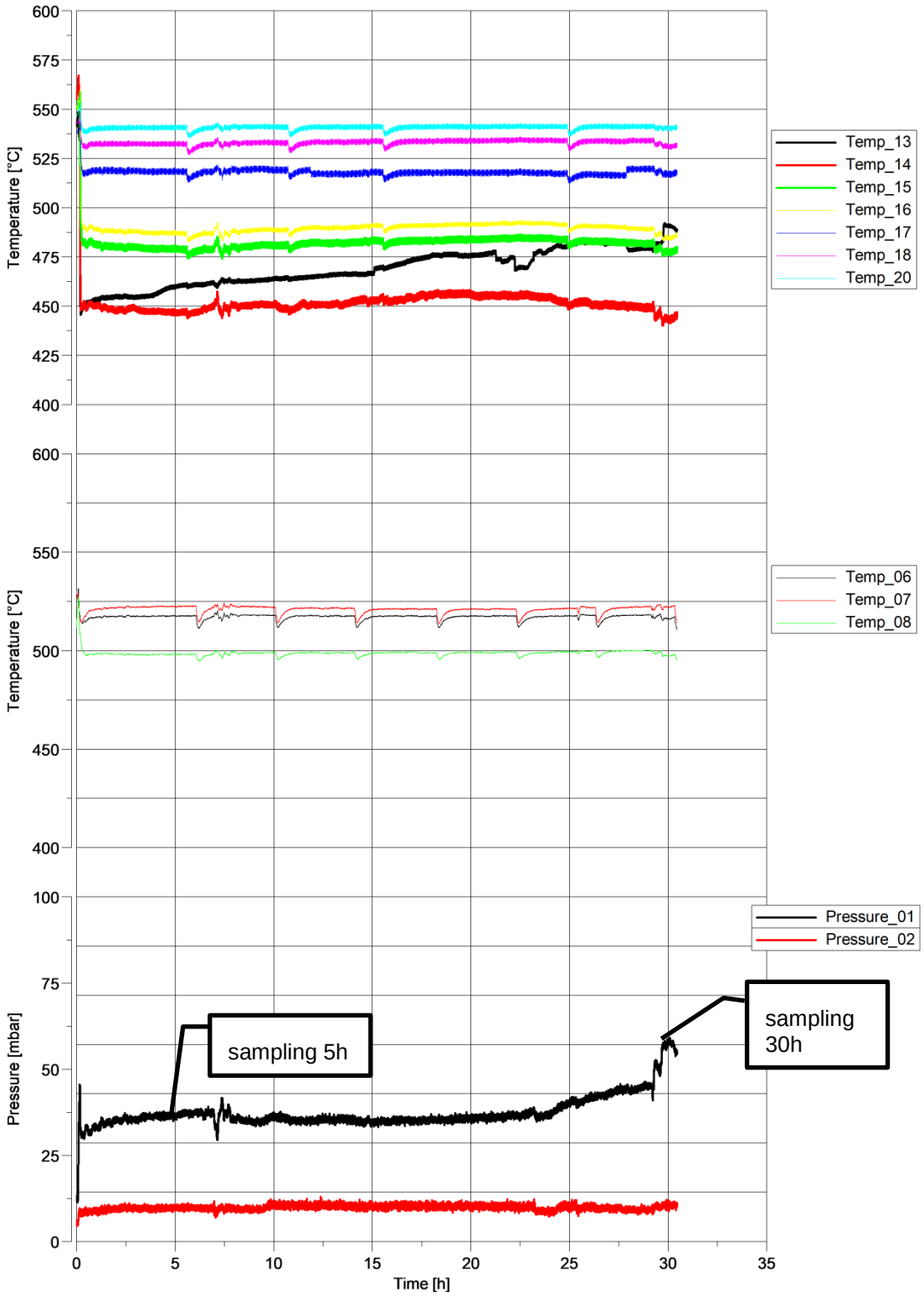

Figure 5.12 Temperature and pressure diagram: S/C 2,5; GHSV 1500;

$\dot{V}_{LPG} = 130\ [Nl/h];\ \dot{V}_{H_2O} = 995\ [Nl/h];\ T_{ref} = 550°C$

5.8 **Summary**

The medium test run was carried out with an S/C-ratio of 2,5 and a GHSV of 1500 1/h both parameters were kept constant. After 5 h and 30 h a sample was taken with a gas bag and afterwards analysed by a micro GC. The measured volume ratios increased slightly over time but compared to the average measured volume ratios regarding the calculated equilibrium the deviation was very small. Furthermore, the temperature range is in accordance with the temperature range in the reformer. Due to the analysis with a GC it was possible to find out whether there were any inlet gas products left in the outlet gas or not. Temperature T13 continuously rose over time, first slowly but then faster by the end of the test time. This increase in temperature is an indicator for a possible increase of the exothermic methanation reaction according equation 2.14 . The rise in temperature correlates with a significant rise in pressure after a test duration of 25 hours, ending with a sudden peak in pressure. As a result, the test was stopped.

6. Conclusion and Outlook

This thesis deals with the evaluation of the most suitable key parameters for steam reforming of LPG on a Nickle based catalyst. The conducted series of tests and the investigation of the test procedure within the framework of process analyses have shown promising results for the steam reforming of LPG. As a result, a range of critical process parameters have been evaluated for safe operation. Additionally, key parameters have been evaluated, which should be further examined in a long run test.

Three test series have been conducted with an S/C-ratios of 1,5 - 3 and a GHSV ranging from 1500 1/h - 3000 1/h; temperature was set at 545°C, which was predefined by previous tests. Thus, it was possible to understand the behaviour of the catalyst in terms of outlet concentration of the components, in terms of conversion rate and carbon formation. However, it must be pointed out that carbon formation is one of the major problems of steam reforming of LPG. Carbon deposition can lead to variety of problems ranging from deactivation to blocking of the active surface, which results in a pressure rise and in an increase in temperature, such as in the extended test series and medium test run. This rise in pressure and temperature is outlined in chapters 5.5 and 5.7. The two final diagrams summarise all tests result.

Table 6.1 Relative pressure difference in the tests

$\Delta p_{relative}$ [mbar]					
S/C [-]	3	✓	✓	X	X
	2,5	✓	X	X	X
	2	X			
	1,5	✓			
		1500	2000	2500	3000
GHSV [1/h]					

Table 6.2 Equilibrium of the tests

Equilibrium					
S/C [-]	3	✓	↓	↓	↓
	2,5	✓	↓↓	↑	↓
	2	↓			
	1,5	↓			
		1500	2000	2500	3000
GHSV [1/h]					

To sum up, an S/C-ratio higher or equal to 2,5 and a GHSV of 1500 1/h are the favourable key parameters at least for 30 h of test duration. The test met the

boundary conditions of 15 Vol - % of CH_4 and an S/C-ratio as low as possible to save heat duty. Furthermore, the temperature range where the equilibrium curve intercepting the measured test results, lies in the operating temperature range of the reformer. The matlab program performed well to forecast the outlet gas mixture when the temperature range was in the operating temperature range of the reformer. This was also shown in the first test series with an S/C-ratio of 3 and a GHSV of 1500 1/h.

However, even the medium test run has also shown that even with an S/C-ratio of 2,5 it could not prevent the catalyst from running in to carbon formation problem at the end of the test. So preferably a higher S/C-ratio e.g. an S/C-ratio of 3 should be chosen for long run tests. It was observed that the catalyst has shown well behaviour in regeneration. After washing the catalyst for several minutes (0,5 h) no more CO_2 was detected and the pressures went back to the original levels.

The conversion rate of the catalyst can be described as very well at least for the tests that were analysed by a GC. It was proven that there are no inlet gas components (C_3H_8 and C_4H_{10}) detected in the outlet gas. Also, no further components of higher and lower hydrocarbons were detected. That is important since higher hydrocarbons such as C_3H_8 and C_4H_{10} cannot be internally reformed in SOFCs.

Carbon formation is one of the major problems in the steam reforming of LPG. I would recommend further tests with chemically pure C_3H_8 and C_4H_{10}. That could lead to a better understanding of the appearance of carbon deposition and a more accurate forecast of the outlet gas mixture. Additionally, carbon formation due to unsaturated hydrocarbons feed could be excluded. LPG is a non-standard gas, so the tests with pure components could lead to a better transferability of key parameters to different LPG mixtures. Finally, some promising values of key parameters have been found, which can be very useful in a multiple fuel combined heat and power system.

7. Appendix

7.1 List of Figures

7.2 List of Tables

7.3 References

[1] D. V. Flüssiggas, „http://dvfg.de/deutscher-verband-fluessiggas-e-v/,“ 29 12 2016. [Online].

[2] „AVL intern“.

[3] W. Winkler, Brennstoffzellenanlagen, Berlin, Heidelber: Springer, 2002.

[4] M. Klell, Höhere Thermodynamik, Graz: Skript. Institut für Verbrennungskraftmaschinen und Thermodynamik (TU Gaz), 2012.

[5] V. Hacker, *Brennstoffzellensysteme, Habiltation, Fakultät für Technische Naturwissenschaftlichen,* Graz: TUGraz, 2003.

[6] H. Timmermann, Untersuchungen zum Einsatz von Reformat aus flüssigen Kohlenwasserstoffen in der Hochtemperaturbrennstofzelle SOFC, Karlsruhe, Deutschland,: KIT Science Publisching, 2009.

[7] J. Lamanie und A. Dicks, Fuel Cell Systems Explained. 2. Edition, Chester: John Wiley & Sons,Ltd, 2003.

[8] Y. Thaller, *Dynamische Moderlierung eines SOFC-Stacks und Reformer,* Graz: Campus 02, 2016.

[9] J. S. D. A. B. D. Shekhawat, Fuel Cell Technologie for fuel processing, Morgan Town, WV, USA: Elsevier Science, 2011.

[10] J. D. Larmanie, Fuel Cell Systems Explained, Chichester: John Wiley & Sons, Ltd, 2003.

[11] S. GmbH, *Mk100-Stack WP507 Produktdatenblatt,* 2007.

[12] R. P. T. A. J. Pasel, Wasserstofferzeugung aus Dieselkraftstoffen, FVS Themen, 2004.

[13] Ö. E. 589, *Automotive fuels_LPG-Requirremants and test methods,* Wien: Austrian Standards Institut, 2009.

[14] Z. Malaibari, Hydrogen Production from Liquefiied Petroleum Gas (LPG) by oxidative Steam Reforming Over Bimetallic Catalysts, Canada, 2011.

[15] S. Anger, Untersuchung zur Prozessgasaufbereitung von Flüssiggas für Dampfreformierung in Brennstoffzellen-BHKW, Freiberg, 2015.

[16] O. Levenspiel, Chemical Reaction Engineering, Bd. 3ed ed., New York: John Wiley & Sons, 1999.

[17] R. D. a. G.Emig, Handbook of Heterogeneous Catalysis, Weinheim: VCH Verlagsgesellschaft, 2008.

[18] Bartholomew, „Mechanisma of catalysr deactivation," Bde. %1 von %2Applied Catalysis A: General, 212, 2001, pp. 12-60.

[19] J. J. Spivey, Fuel Cells: Technologies for Fuel Processing, Louisiana State University: Elsevier, 2011, pp. pp.317-360.

[20] R.-N. J.R., Catalytic Steam Reforming, Catalysis Science and Techology, Bd. Volume 5, New York: Springer, 1984, pp. pp. 1-117.

[21] D.L.Trimm, Catal. Rev.Sci. Eng, 1977.

[22] J. C. J.R. Rostrup-Nielson and D.L.Trimm, 1997.

[23] J. G. K. F. K.Ahmed, „Demonstration of LPG-fueled solide oxide fuel cell systems," *Solide State Ionics ,* pp. 485-492, 18 January 2002.

[24] X. W. Xiujing Zou, „Development of highly effective supported nickel catalysts for pre-reforming of liquefied petroleum gas under low steam to carbon molar ratios," Shanghai, China, 2010.

[25] Y. T. A. N. Katsutoshi Sato, „Dual fuel type solide oxide fuel cell using dimethyl ether and liquefied petroleum gas as fuels," *Journal of Power Sources 217,* pp. 37-42, 2012.

[26] Clariant, Interviewee, [Interview]. 2016.

[27] S. A. N. Laosiripojana, „Hydrogen production from steam and authothermal reforming of LPG over high sureface area ceria," Journal of Power Sources 158, Thailand, 2006.

[28] J. Hirschenhofer, D. Stauffer, R. Engleman und Klett, Fuel Cell Handbook. 4. Ausgabe, 1998.

[29] A. N. Jennifer Oppel, Klimawandel-Eine Herausforderung für die Wirtschaft: Handlungsoptionen für Industrieunternehmen in Deutschalnd, Hamburg: Diplom.de, 2008.

[30] A. Konnov, Detailed reaction mechanism for small hydroarbons combustion Release 0.5, Brüssel: Fifth Recearch Framework Rogramm (FP5), 2006.

[31] M. Dr. Hauth, Interviewee, *AVL*. [Interview]. 2017.

[32] D. S. R. E. a. M. K. J.H.Hirschenhofer, Fuel Cell Handbook Fouth Edition, Morgantown, WV: U.S Department of Energie, 1998.

8. Appendix

8.1 Calibration curve

The task was to evaluate $\dot{V}_{soll}$ that describes the volume flow which is set by the *LabView* program. $\dot{V}_{gil}$ is the measured volume flow by the *Gilibrator -2.*

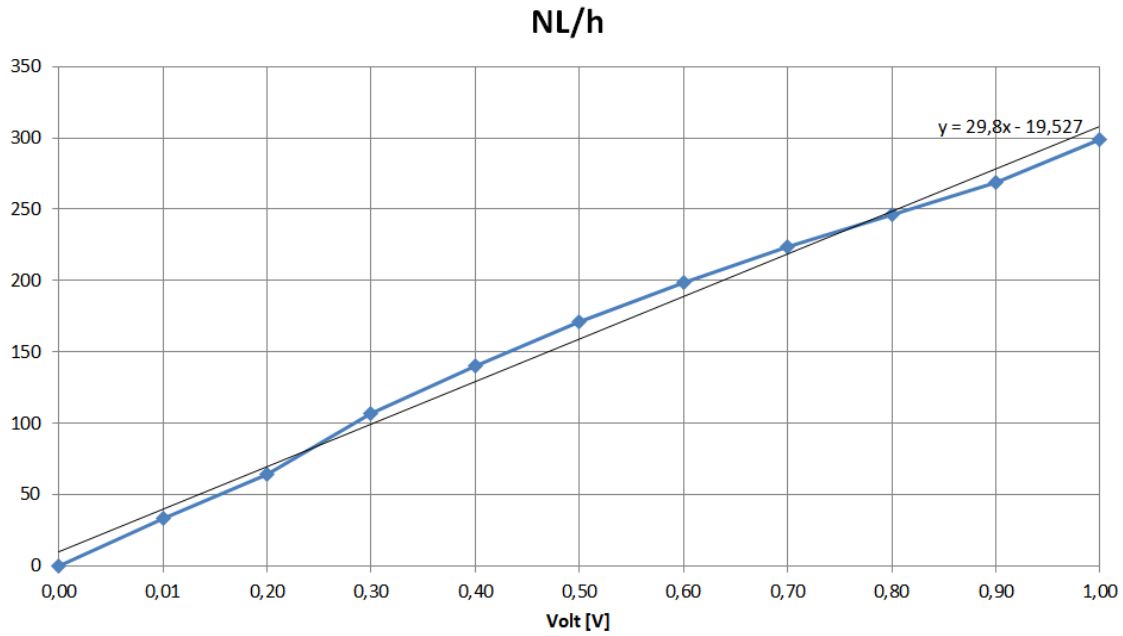

Figure 8.1 Calibrations curve LPG

Table 8.1 Measured data for calibration curve LPG

			p1=p2	101300	Pa
			T1	273,15	K
	Mass Flow LPG		T2	278,15	K
			V1	V2	V2
Meas.	Volt [V]	[cc/m]	V1 [l/min]	[Nl/min]	[Nl/h]
1	0,00	0,00	0,00	0,00	0,00
2	0,01	0,00	0,00	0,00	33,00
3	0,20	1045,00	1,05	1,06	64,00
4	0,30	1745,00	1,75	1,78	107,00
5	0,40	2285,00	2,29	2,33	140,00
6	0,50	2800,00	2,80	2,85	171,00
7	0,60	3254,00	3,25	3,31	199,00
8	0,70	3665,00	3,67	3,73	224,00
9	0,80	4024,00	4,02	4,10	246,00
10	0,90	4405,00	4,41	4,49	269,00
11	1,00	4900,00	4,90	4,99	299,00

8.2 **Amount of carbon deposition**

How much carbon is dispositioned in the catalyst can be theoretically calculated by a carbon balance in the system. It is the difference between the feed gas which contains (C_3H_8 and C_4H_{10}) and the outlet gas (CO, CO_2, CH_4). The

amount of depositioned carbon in gram per catalyst can be expressed by the following equation [27]:

$$C_{dep.} = \frac{n_{carbon\,(in)} - n_{carbon\,(out)}}{m_{catalyset}} \quad \left[\frac{mol}{g}\right] \qquad \text{Equation 8.1}$$

8.3 **Calculations of the water and LPG amount**

The calculations have been done in excel. For the calculations it was necessary to insert the S/C – ratio and the GHSV as well as catalyst volume

Catalyst volume = 0,75 dm^3

standard conditions for temperature and pressure:

$p_s = 1{,}013 * 10^5$ Pa

T = 273,15 K

Given: S/C

GHSV

$$\frac{S}{C} = \frac{n_{H_2O}}{x * n_{LPG}} \rightarrow x_{LPG} \quad [-] \qquad \text{Equation 8.2}$$

$$n_{LPG} = \sum x_i * n_{c_x} \quad [mol] \qquad \text{Equation 8.3}$$

$$1 = x_{H_2O} + x_{LPG} \rightarrow x_{H_2O} \quad [-] \qquad \text{Equation 8.4}$$

$$\dot{V}_{total} = GHSV * V_{cat.} \quad \left[\frac{Nm^3}{h}\right] \qquad \text{Equation 8.5}$$

$$\dot{V}_{LPG} = \dot{V}_{total} * x_{LPG} \quad \left[\frac{Nm^3}{h}\right] \qquad \text{Equation 8.6}$$

$$\dot{V}_{H_2O} = \dot{V}_{total} * x_{H_2O} \quad \left[\frac{Nm^3}{h}\right] \qquad \text{Equation 8.7}$$

$$\dot{m}_{H_2O} = \frac{p_s * \dot{V}_{H_2O}}{\frac{R}{M_{H_2O}} * T} \quad \left[\frac{g}{h}\right] \qquad \text{Equation 8.8}$$

8.4 Temperature distribution over catalyst length

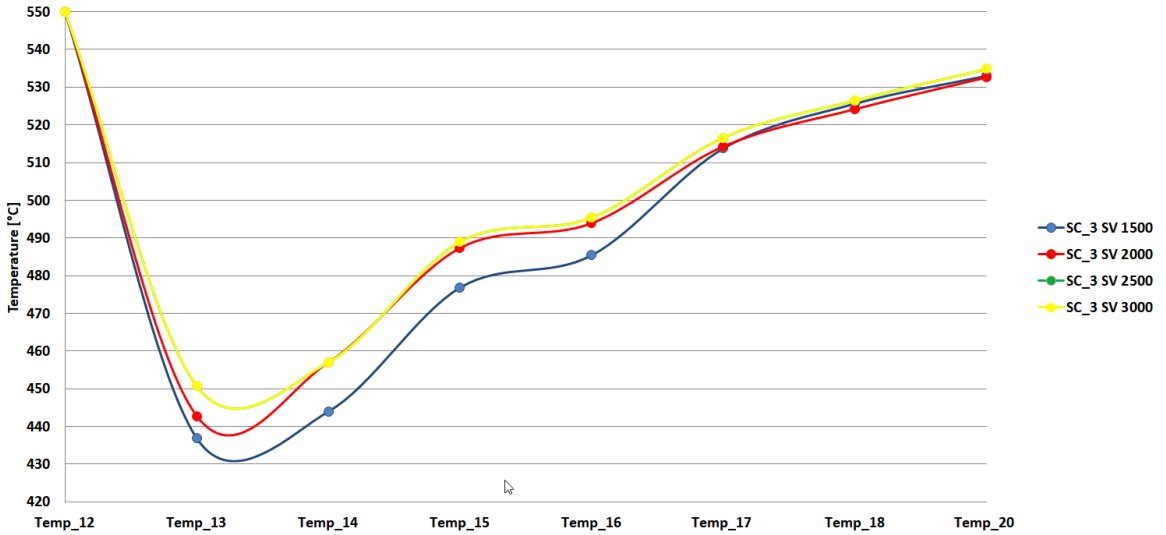

Figure 8.2 Temperature distribution of the 1. test series from thermocouple T12 – T20

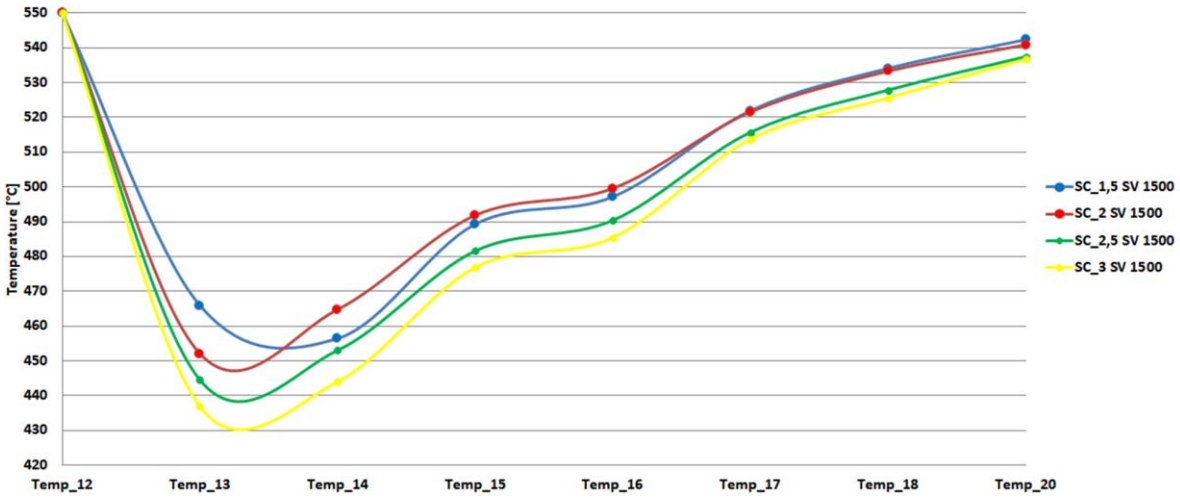

Figure 8.3 Temperature distribution of the 2. test series from thermocouple T12 – T20

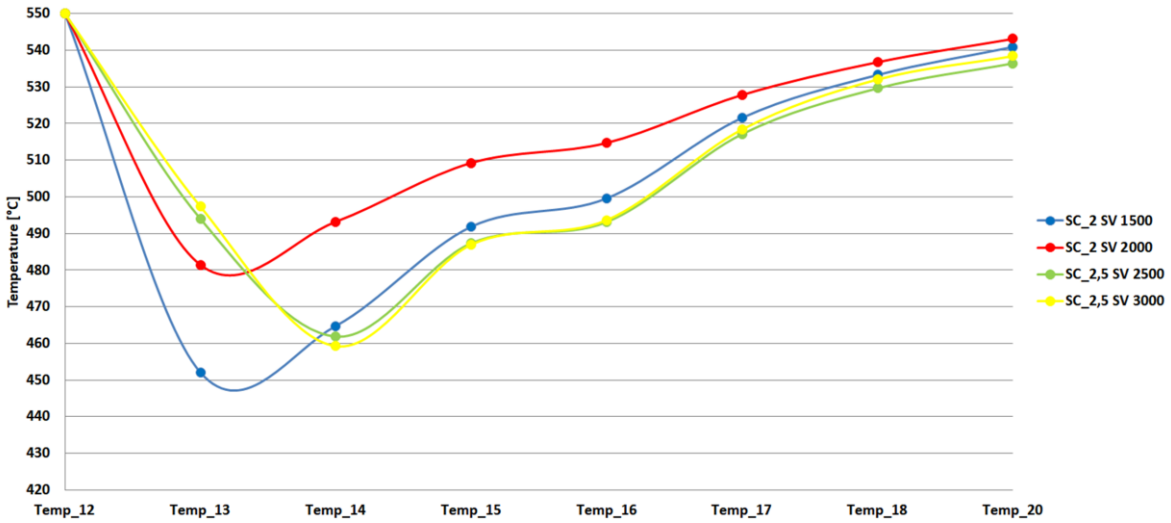

Figure 8.4 Temperature distribution of the extended test series from thermocouple T12 – T20

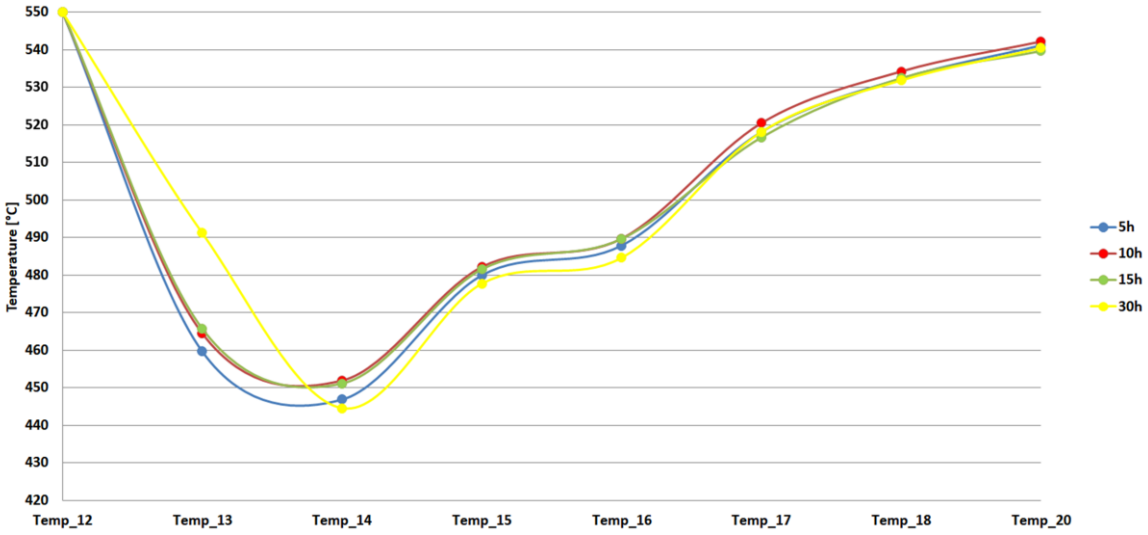

Figure 8.5 Temperature distribution of the medium test run from thermocouple T12 – T20

8.5 Pressure p_1 over volume flow

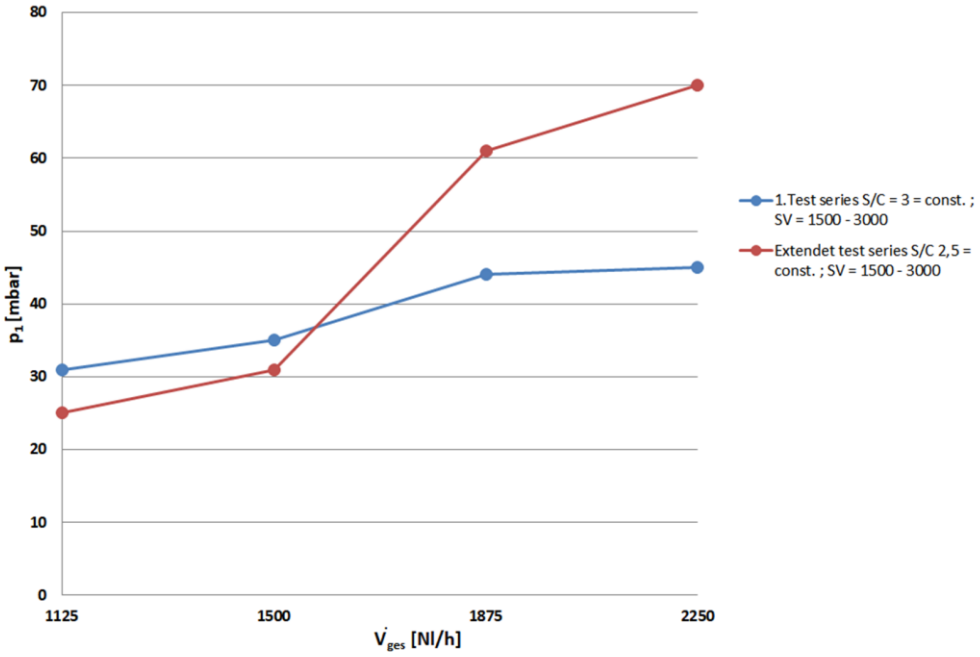

Figure 8.6 p_1 over norm flow rate

8.6 **Reforming tests**

Table 8.2 Overview of the reforming tests

Diesel tests	Date	S/C	SV	T_{ref} [°C]	LPG [Nl/h]	H_2O [Nl/h]	status
	24.10.2016	2,5	1200	550	x	x	failed test
	25.10.2016	2,5	1200	550	820	800	ok
	03.11.2016	2,5	1200	550	820	800	ok
	04.11.2016	2,5	1200	550	820	800	ok
	11.11.2016	2,2	1200	550	820	797	ok
LPG test	1.Test series		new cata-lyst				
	29.11.2016	3	1500	550	x	x	failed test
	30.11.2016	3	1500	550	x	x	failed test
	06.12.2016	3	1500	550	111	1014	ok
	07.12.2016	3	2000	550	148	1352	ok
	13.12.2016	3	2500	550	185	1690	ok
	15.12.2016	3	3000	550	222	2028	ok
	2. Test series						
	02.02.2017	1,5	1500	550	202	923	ok
	14.12.2016	2	1500	550	158	967	ok
	09.12.2016	2,5	1500	550	130	995	ok

	29.11.2017	3	1500	550	111	1014	ok
	Extended test series						
	14.02.2017	2,5	2000	550	174	1326	ok
	16.02.2017	2,5	2500	550	217	1658	ok
	21.02.2017	2,5	3000	550	261	1989	ok
	Medium test run 30 h						
	22.02.2017	2,5	1500	550	130	995	ok
	23.02.2017						
	24.02.207						

9. Appendix

9.1 Temperature and pressure diagrams

1.Test series

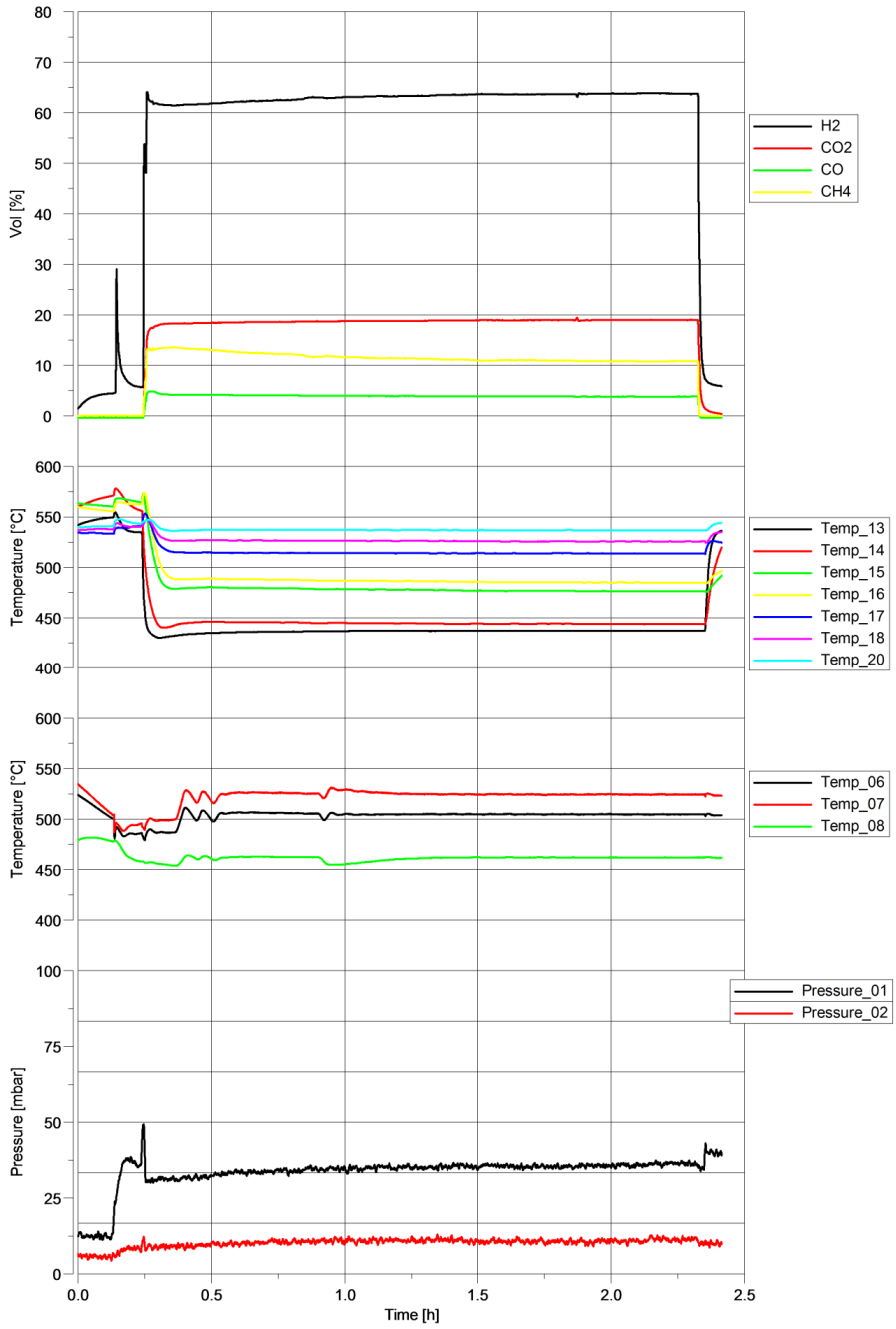

Figure 9.1 Temperature and pressure: S/C 3; GHSV 1500;

$$\dot{V}_{LPG} = 111\ [Nl/h];\ \dot{V}_{H_2O} = 1014\ [Nl/h];\ T_{ref} = 550°C$$

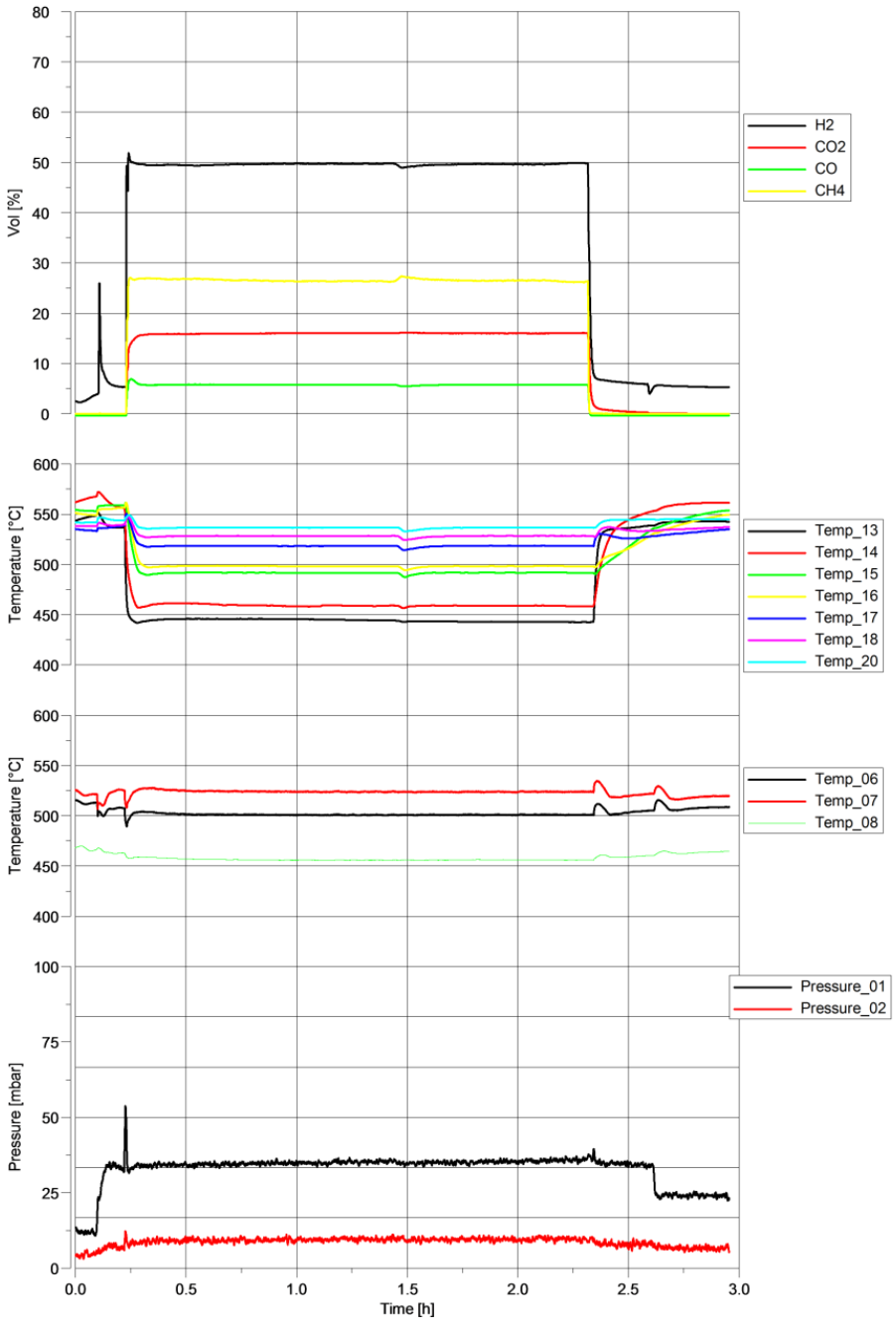

Figure 9.2 Temperature and pressure diagram: S/C 3; GHSV 2000;

$\dot{V}_{LPG} = 148\ [Nl/h];\ \dot{V}_{H_2O} = 1352\ [Nl/h];\ T_{ref} = 550°C$

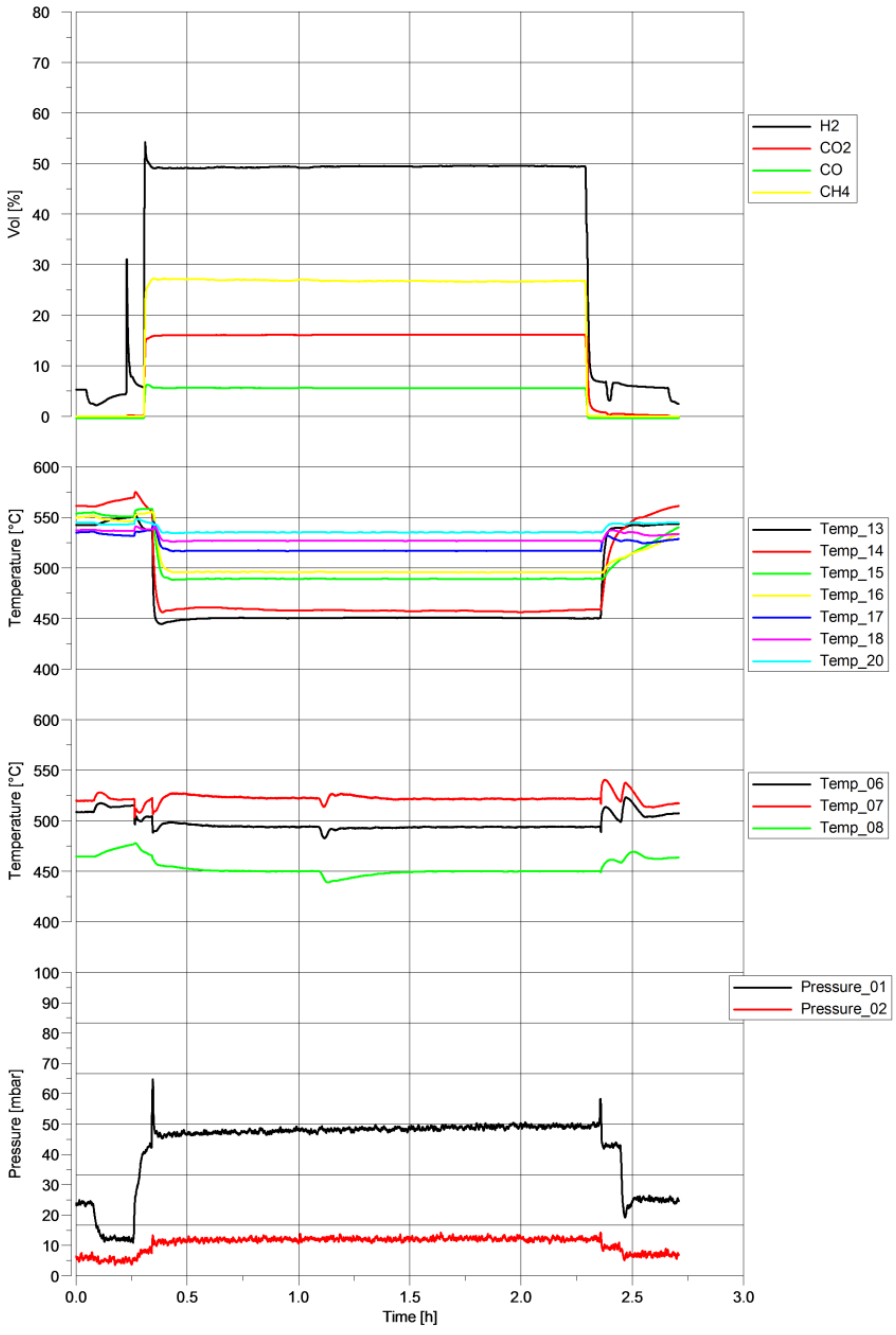

Figure 9.3 Temperature and pressure diagram: S/C 3; GHSV 2500;

$\dot{V}_{LPG} = 185\ [Nl/h];\ \dot{V}_{H_2O} = 1690\ [Nl/h];\ T_{ref} = 550°C$

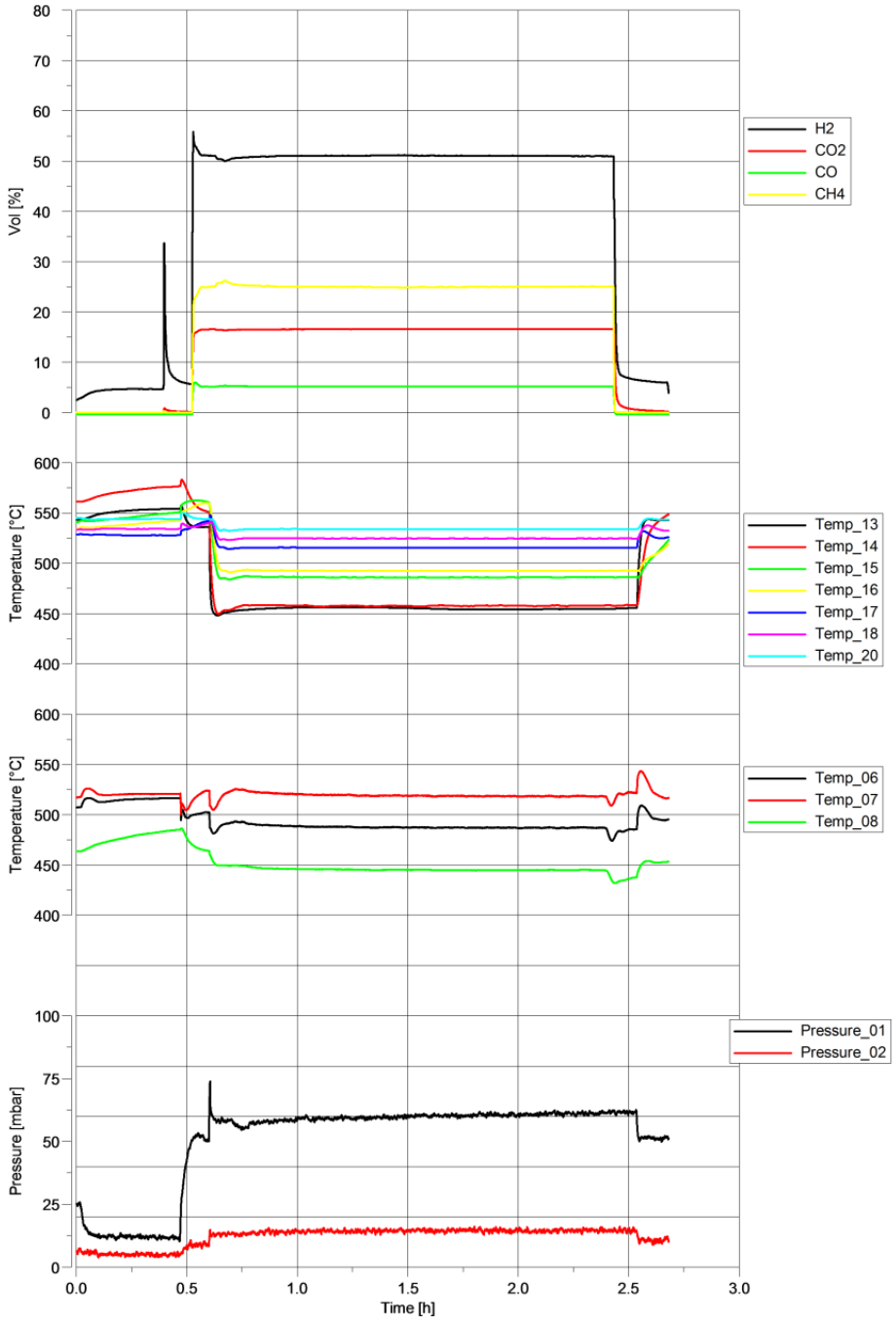

Figure 9.4 Temperature and pressure diagram: S/C 3; GHSV 3000;

$\dot{V}_{LPG} = 222\ [Nl/h];\ \dot{V}_{H_2O} = 2028\ [Nl/h];\ T_{ref} = 550°C$

2. Test series

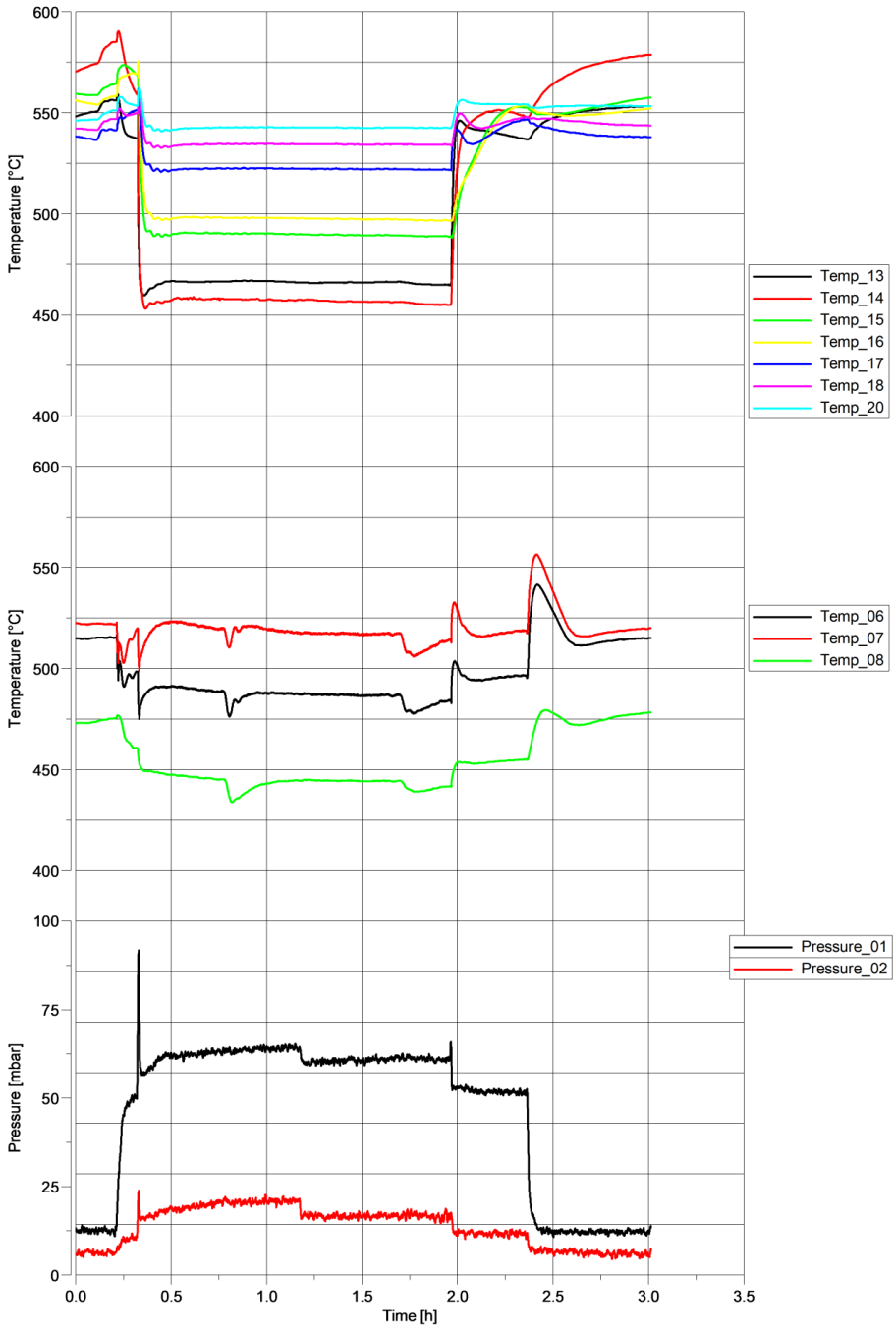

Figure 9.5 Temperature and pressure diagram: S/C 1,5; GHSV 1500;

$$\dot{V}_{LPG} = 202\ [Nl/h];\ \dot{V}_{H_2O} = 923\ [Nl/h];\ T_{ref} = 550°C$$

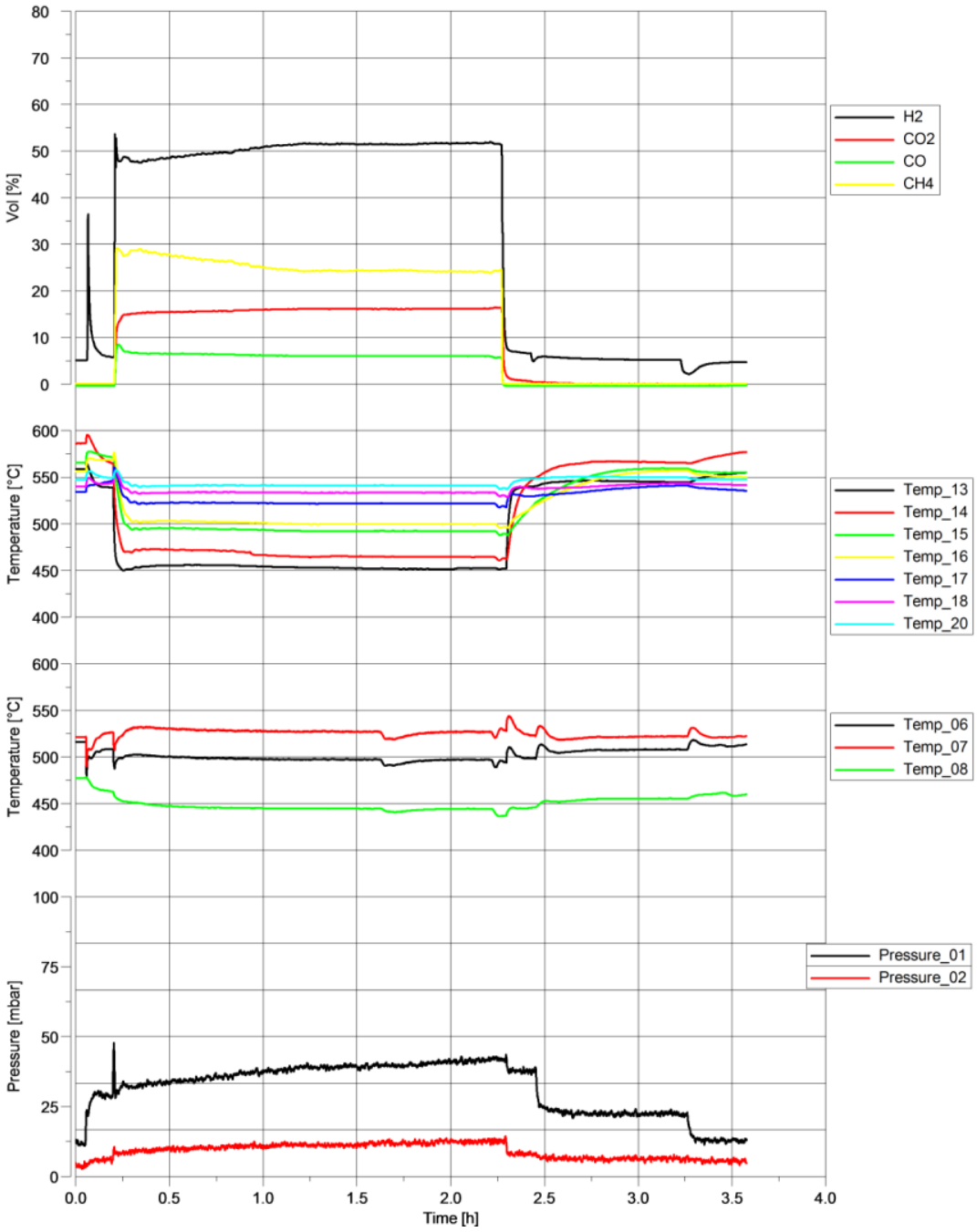

Figure 9.6 Temperature and pressure diagram: S/C 2; GHSV 1500;

$\dot{V}_{LPG} = 158\ [Nl/h];\ \dot{V}_{H_2O} = 967\ [Nl/h];\ T_{ref} = 550°C$

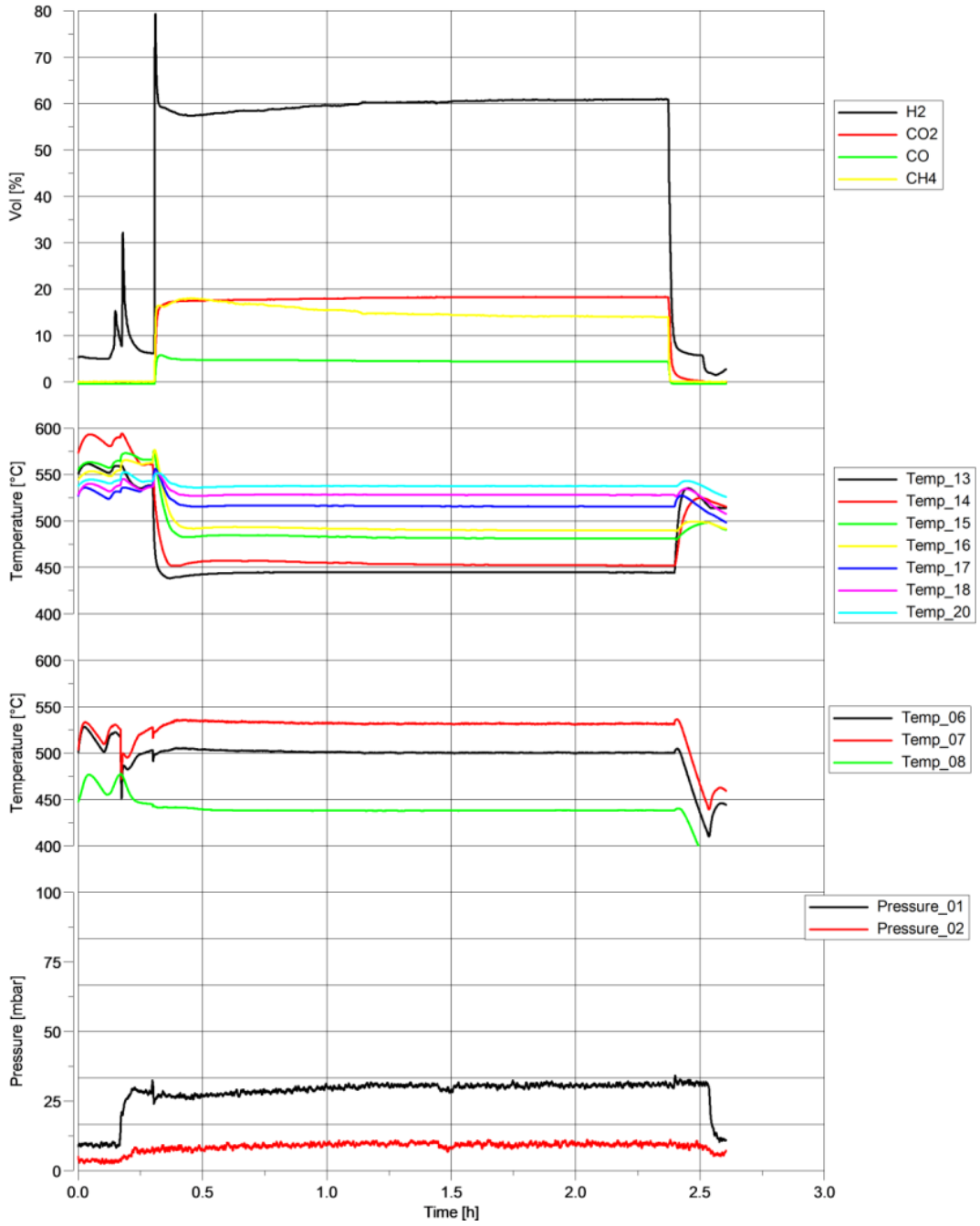

Figure 9.7 Temperature and pressure diagram: S/C 2,5; GHSV 1500;

$\dot{V}_{LPG} = 130\ [Nl/h];\ \dot{V}_{H_2O} = 995\ [Nl/h];\ T_{ref} = 550°C$

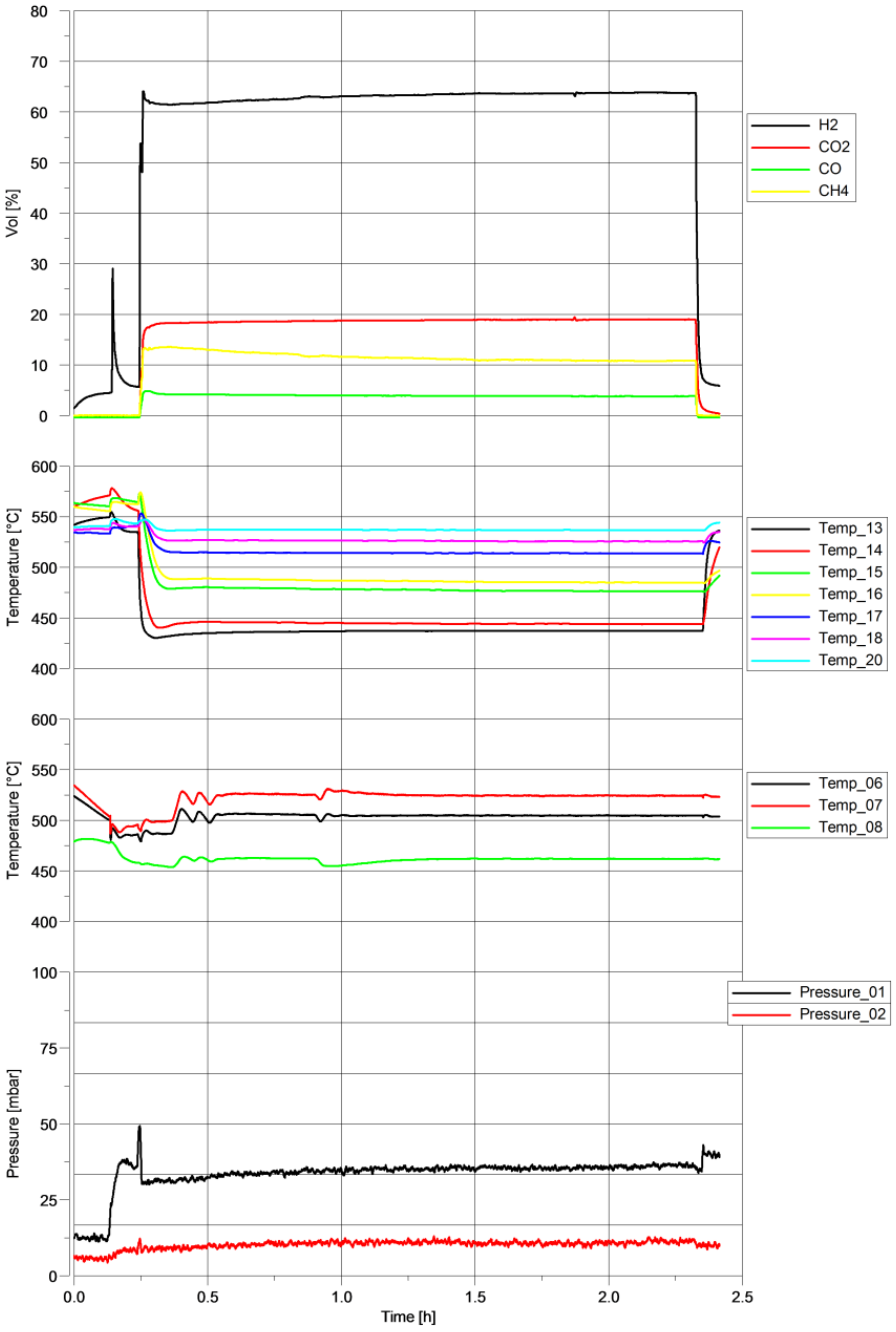

Figure 9.8 Temperature and pressure diagram: S/C 3; GHSV 1500;

$$\dot{V}_{LPG} = \ 111\ [Nl/h];\ \dot{V}_{H_2O} = 1014\ [Nl/h];\ T_{ref} = 550°C$$

Extended test series

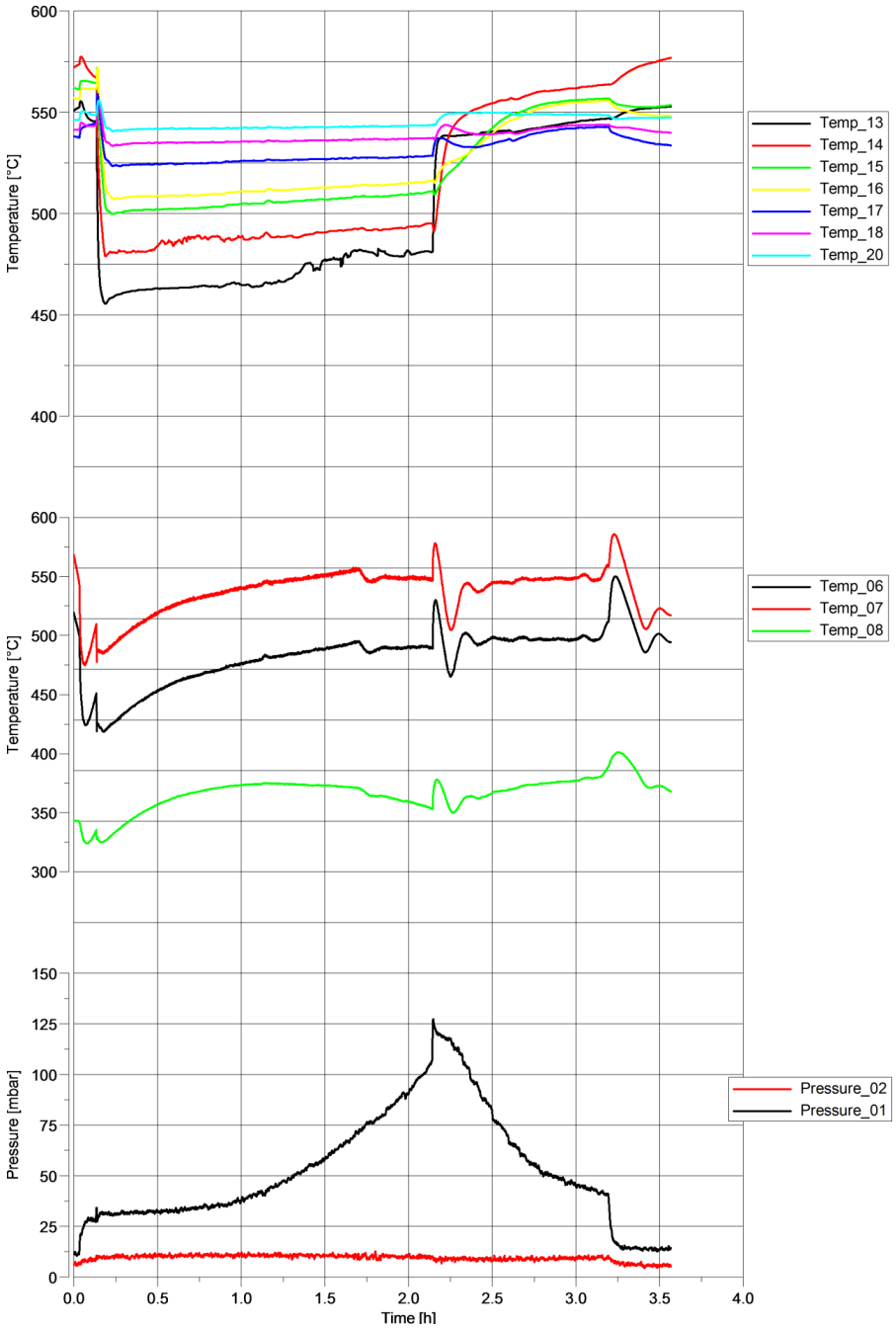

Figure 9.9 Temperature and pressure diagram: S/C 2,5; GHSV 2000;

$$\dot{V}_{LPG} = \ 174\ [Nl/h];\ \dot{V}_{H_2O} = 1326\ [Nl/h];\ T_{ref} = 550°C$$

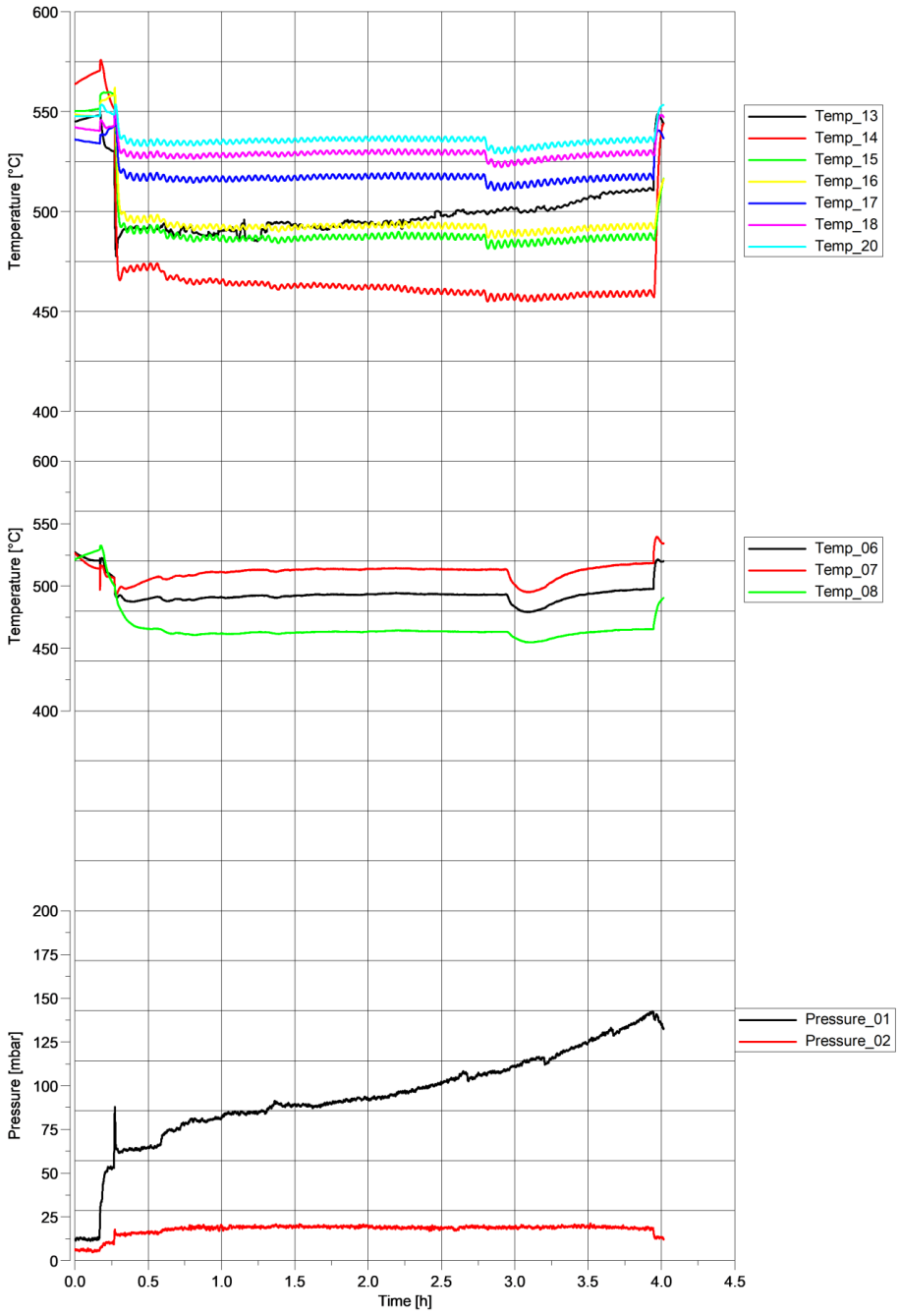

Figure 9.10 Temperature and pressure diagram: S/C 2,5; GHSV 2500;

$$\dot{V}_{LPG} = 217\ [Nl/h];\ \dot{V}_{H_2O} = 1658\ [Nl/h];\ T_{ref} = 550°C$$

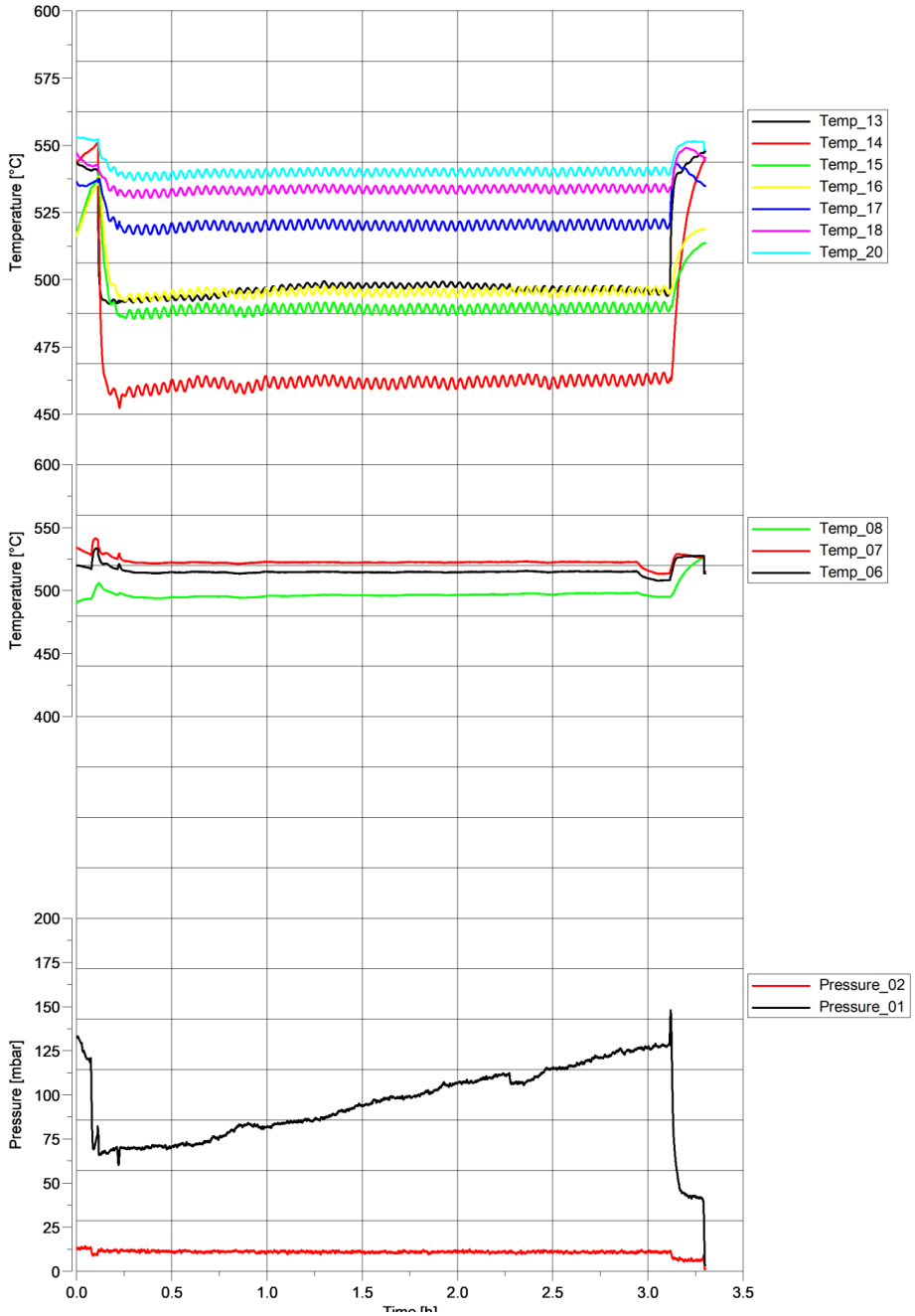

Figure 9.11 Temperature and pressure diagram: S/C 2,5; GHSV 3000;

$\dot{V}_{LPG} = 261\ [Nl/h];\ \dot{V}_{H_2O} = 1989\ [Nl/h];\ T_{ref} = 550°C$

Medium test run

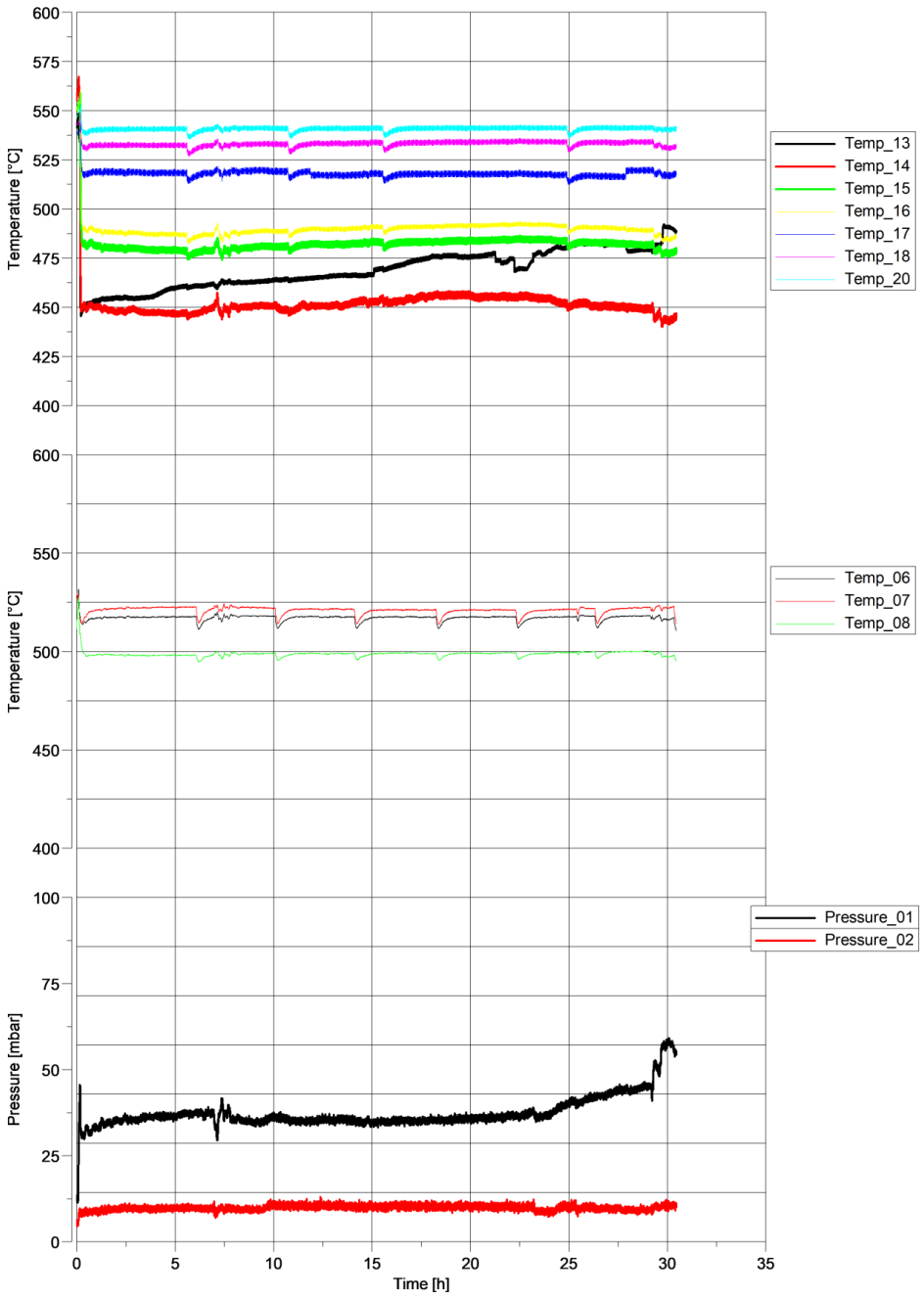

Figure 9.12 Temperature and pressure diagram S/C 2,5; GHSV 1500;

$$\dot{V}_{LPG} = 130\ [Nl/h];\ \dot{V}_{H_2O} = 995\ [Nl/h];\ T_{ref} = 550°C$$